Atmos. Chem. Phys. Discuss., doi:10.5194/acp-2017-131, 2017
Manuscript under review for journal Atmos. Chem. Phys.
Discussion started: 16 February 2017

Atmospheric Chemistry and Physics Discussions

Seasonal provenance changes of present-day Saharan dust collected on- and offshore Mauritania

Carmen A. Friese[1], Hans van Hateren[2,*], Christoph Vogt[1,3], Gerhard Fischer[1], Jan-Berend W. Stuut[1,2]

[1]Marum-Center of Marine Environmental Sciences, University of Bremen, Bremen, 28359, Germany
[2]NIOZ-Royal Netherlands Institute for Sea Research, Department of Ocean Systems, and Utrecht University, 1790 AB, Den Burg Texel, Netherlands
[3]ZEKAM, Crystallography, Geosciences, University of Bremen, 28359, Germany
[*]Now at: Vrije Universiteit Amsterdam, Faculty of Earth Sciences, 1081 HV Amsterdam, the Netherlands

Correspondence to: Carmen A. Friese (cfriese@marum.de)

Abstract.

Saharan dust has a crucial influence on the earth climate system and its emission, transport, and deposition are intimately related to environmental parameters. The alteration in the physical and chemical properties of Saharan dust due to changes in environmental parameters is often used to reconstruct the climate of the past. However, to better interpret possible climate changes the dust source regions need to be known. By analysing the mineralogical composition of transported or deposited dust, potential dust source areas can be inferred. Summer dust transport offshore Northwest Africa occurs in the Saharan air layer (SAL). In contrast, dust transport in continental dust source areas occurs predominantly with the trade winds. Hence, the source regions and related mineralogical tracers differ with season and sampling location. To test this, dust collected in traps onshore and in oceanic sediment traps offshore Mauritania during 2013 to 2015 was analysed. Meteorological data, particle-size distributions, back-trajectory and mineralogical analyses were compared to derive the dust provenance and dispersal. For the onshore dust samples, the source regions varied according to the seasonal changes in trade-wind direction. Gibbsite and dolomite indicated a Western Saharan and local source during summer, while chlorite, serpentine and rutile indicated a source in Mauritania and Mali during winter. In contrast, for the samples that were collected offshore, dust sources varied according to the seasonal change in the dust transporting air layer. In summer, dust was transported in the SAL from Mauritania, Mali and Libya as indicated by ferryglaucophane and zeolite. In winter, dust was transported with the Trades from the Western Sahara as indicated by e.g. sepiolite and fluellite.

Keywords

Saharan dust, MWAC, sediment trap, mineralogy, particle size, major potential source area, provenance

Atmos. Chem. Phys. Discuss., doi:10.5194/acp-2017-131, 2017
Manuscript under review for journal Atmos. Chem. Phys.
Discussion started: 16 February 2017

Atmospheric Chemistry and Physics Discussions

1 Introduction

Mineral dust influences global climate through many feedback mechanisms and is in turn influenced by variations in environmental parameters. The emission, transport and deposition of mineral dust reacts sensitively to parameters of climate change like rainfall, wind, temperature and vegetation cover (Knippertz and Stuut, 2014). In turn, the emission, transport and deposition of mineral dust has an impact on the atmospheric energy balance (Haywood and Boucher, 2000), precipitation distribution and amplitude (Yoshioka et al., 2007), sea surface temperatures (Lau and Kim, 2007) as well as the oceanic carbon pump (Martin, 1990;Martin et al., 1991;Jickells et al., 2005;Ploug et al., 2008a;Iversen et al., 2010;Iversen and Robert, 2015). The sensitivity of mineral dust to environmental parameters is used to reconstruct the climate of the past (Diester-Haass and Chamley, 1978;Stein, 1985;Rea, 1994;Holz et al., 2007;Tjallingii et al., 2008;Mulitza et al., 2010). For instance, the particle size of mineral dust in ocean sediment records varies according to the paleo-frequency of dust-storm and rainfall events (e.g., (Friese et al., 2016). Further, the mineralogical composition of mineral dust in sediment core records can be used as a qualitative proxy for the paleo-dust source activity (Scheuvens et al., 2013).

Every year, about 2000Mt dust are emitted from source areas around the world, of which 75% are deposited on land and 25% into the oceans (Shao et al., 2011).The Saharan Desert is the world's largest source of mineral aerosols with an annual dust transport of ~180 Mt westwards towards the North Atlantic (Yu et al., 2015). About 140Mt is actually deposited into the North Atlantic Ocean (Yu et al., 2015). In addition, about 430 Mt is blown from the Sahara towards the equatorial Atlantic (Shao et al., 2011) and therefore constitutes an essential component of the global climate system. The source regions of Saharan dust have been studied frequently by analysing the mineralogical composition of dust collected at continental sites (e.g.(Schütz and Sebert, 1987;Khiri et al., 2004;Kandler et al., 2009;Skonieczny et al., 2011;Skonieczny et al., 2013), during aircraft flights (e.g.(Formenti et al., 2008), on research ships (Chester et al., 1971;Chester and Johnson, 1971a;Chester and Johnson, 1971b;Chester et al., 1972;Aston et al., 1973;Stuut et al., 2005) and with gravity cores offshore NW Africa (Biscaye, 1964;Biscaye, 1965;Griffin et al., 1968;Rateev et al., 1969;Diester-Haass and Chamley, 1978;Lange, 1982;Meyer et al., 2013). Continental dust studies in northern Morocco revealed that dust is produced predominantly locally (Khiri et al., 2004;Kandler et al., 2009). For instance, a high percentage of quartz and feldspar and a low amount of micas in the dust samples was interpreted to represent mostly local dust sources and the availability of calcite sources from proximal coastal dunes in Morocco (Khiri et al., 2004). Further, also in Morocco, dust was sampled in Tinfou at a height of 4 m during the SAMUM 2006 field campaign. These samples were analysed for their physical and chemical properties. The particle size correlated to local surface wind speed suggesting the contribution of local dust (Kandler et al., 2009). In contrast, in coastal Senegal dust is sourced by the Sahel during winter as shown by low illite/kaolinite (I/K) ratios and lower palygorskite contents as opposed to the summer samples which were suggested to be originating from the Sahara (Skonieczny et al., 2013). Further, the I/K ratio in dust sampled on the Cape Verde Islands showed that dust was derived from strongly varying sources: north-western Sahara, central and southern Sahara and the Sahel (Caquineau et al., 2002). Hence, dust collected on land is predominantly of local provenance, while the sources of dust sampled offshore NW Africa are of regional and long-distance provenance. As a result, a large seasonal difference can be expected in the composition of the marine climate archives, related to the different dominating transport mechanisms of dust in summer and winter (Friese et al., 2016).

Atmos. Chem. Phys. Discuss., doi:10.5194/acp-2017-131, 2017
Manuscript under review for journal Atmos. Chem. Phys.
Discussion started: 16 February 2017

Atmospheric Chemistry and Physics Discussions

To test this, we compared the mineralogical composition, the fluxes, and the particle size of Saharan dust sampled from 2013-2015 in Iwik (Mauritania) in on-land dust traps with Saharan dust sampled from 2013-2015 offshore Cape Blanc (Mauritania) in sub-marine sediment traps. By comparing the data with meteorological data, back trajectories, the African lithology and satellite images we aim to address the following questions:

1) Is there a seasonal variation in the transport patterns of dust deposited on land?
2) What are the source regions of dust trapped on land versus dust trapped in the ocean?
3) Do these source regions vary seasonally?
4) Can we identify characteristic minerals that constitute a tracer for certain source areas?

1.1 North African dust sources

The major potential source areas (PSA) of northern African dust are summarized in a review by Scheuvens et al. (2013), see Fig. 1). Predominant dust transport towards western Africa and offshore the Atlantic Ocean occurs from the foothills of the Atlas mountains, Western Sahara and Western Mauritania (**PSA 2**), southern Algeria and northern Mali (**PSA 3**) and Western Chad including the Bodélé depression (**PSA 5**) (Scheuvens et al., 2013). In contrast, dust sourced from Tunisia and northern Algeria (**PSA 1)** is transported predominantly to the western Mediterranean and Western Europe (Stuut et al., 2009). Central Libya (**PSA 4**) is the most important region for dust transport to the eastern Mediterranean (Scheuvens et al., 2013).

Atmos. Chem. Phys. Discuss., doi:10.5194/acp-2017-131, 2017
Manuscript under review for journal Atmos. Chem. Phys.
Discussion started: 16 February 2017

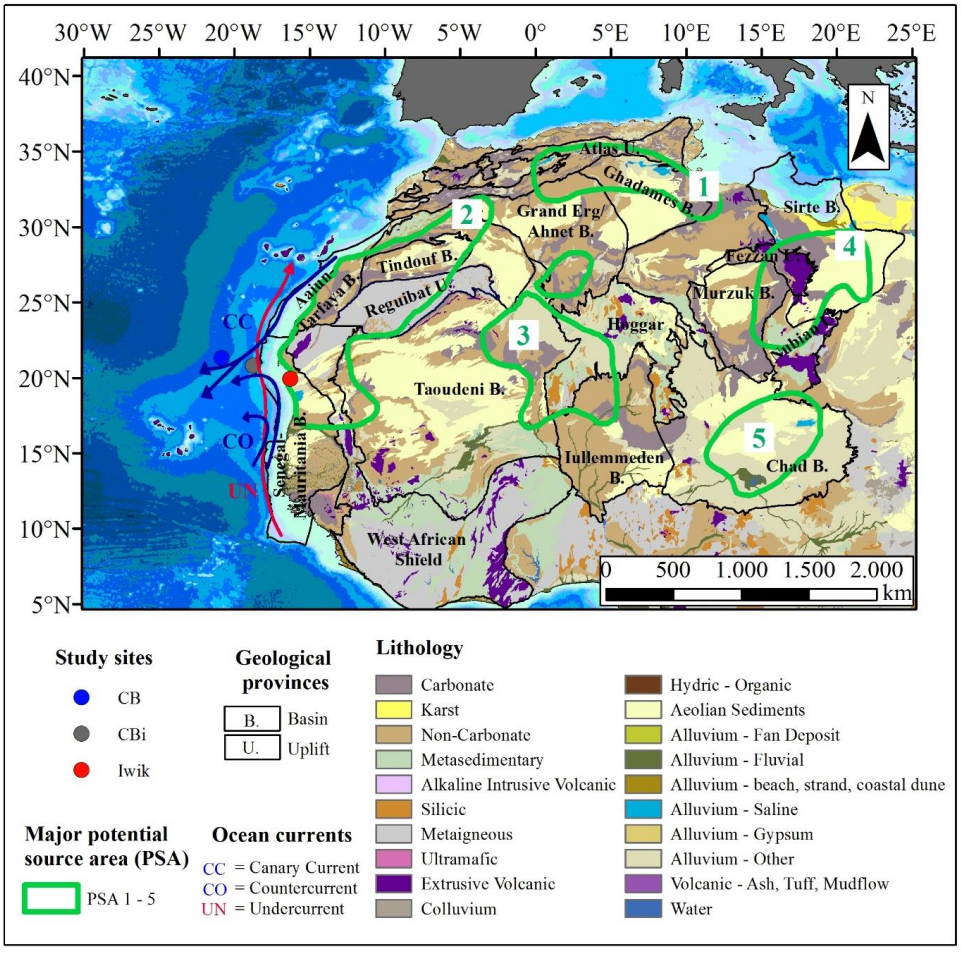

Figure 1: Location of the sediment trap moorings CB and CBi offshore Cape Blanc and the MWAC dust collector on shore near Iwik (shapefile of the surface lithology and the geological provinces: downloaded from the USGS website http://rmgsc.cr.usgs.gov/ecosystems/africa.shtml#SL and http://certmapper.cr.usgs.gov/geoportal/catalog/main/home.page, major potential dust source areas: redrawn from Scheuvens et al. (2013), ocean currents: redrawn from Mittelstaedt (1991)).

1.2 Geological characterisation of dust-producing areas

In the following the lithology of the geological provinces that underlay the major PSA's is outlined (Fig. 1).

The **PSA 1** is underlain by the eastern Atlas chain and the northern Grand erg/Ahnet and Ghadames Basins. The outcrops in the Atlas uplift are composed of e.g. limestones, sandstones and evaporites (Piqué, 2001). The thick strata overlying the northern Ahnet and Ghadames Basin consist of e.g. sandstones and mudstones (Selley, 1997a).

The **PSA 2** is underlain by the Reguibat Shield, the Mauritanides and the Senegal-Mauritania, Aaiun-Tarfaya, Tindouf and Taoudeni Basins. The western part of the Reguibat Shield is dominated by granitic rocks, while the

eastern part is dominated by metamorphic and granitic rocks (Schofield et al. (2006) and references therein). West of the Reguibat Shield, the Mauritanides consist of a metamorphic belt and ophiolite (Villeneuve, 2005). West of the Taoudeni Basin, the Mauritanides are characterized by granites, quartzites and strongly metamorphosed rocks (Villeneuve, 2005). While the Aaiun-Tarfaya Basin features outcrops with dolomites and limestones, the Senegal-Mauritania Basin is characterized by very few carbonate deposits (Bosse and Gwosdz, 1996). The Tindouf Basin is characterized by mainly sandy deposits (Selley, 1997b, a).

The **PSA 3** is underlain by the western Hoggar and parts of the Ahnet, Taoudeni and Iullemeden Basins. The Pharusian belt located in the western Hoggar is characterized by Eburnean granulites, gneiss, graywackes and magmatic rocks (Boullier, 1991). In the southern Ahnet Basin sandstone strata crop out. On the eastern edge of the Taoudeni Basin outcropping sediments are characterized by conglomerates, sandstones and limestones (Bertrand-Sarfati et al., 1991). The outcrops of the Iullemeden Basin are composed of e.g. sandstones, carbonaceous shale, laterites and massive clays (Kogbe, 1973).

The **PSA 4** is underlain by parts of the Fezzan and Nubian uplifts and the Sirte and Murzuk Basins. The eastern Fezzan uplift consists of ocean island basalts (Cvetković et al., 2010;Abdel-Karim et al., 2013), while sediments outcropping in the northern Nubian uplift are composed of e.g. sandstones, limestones and gypsiferous horizons (El Makkrouf, 1988). The southern Sirte Basin is covered by sands, gravel and sand seas (Selley, 1997c). Outcrops of the eastern Murzuk Basin are composed of marine limestones and alluvial sandstones (Selley, 1997a, b).

The **PSA 5** is underlain by the Chad Basin. During the Holocene, the Chad Basin was filled with fine-grained particles from the drainage of the Tibesti mountains to the north (Prospero et al., 2002). Hence, the sediments that outcrop in the central Chad Basin are characterized by fluvial and alluvial sediments such as laminated diatomites, pelites and coastal sandridges (Schuster et al., 2009).

The continental dust collector Iwik (~19°53' N, ~16° 18' W) is located in **PSA 2** in the Parc National de Banc d'Arguin (PNBA) near Iwik in Mauritania (Fig. 1). The local soils surrounding the dust collector are composed of sandy deposits often rich in fossil shells and partly cemented by lime (Einsele et al., 1974).

1.3 Atmospheric setting

Saharan dust emission, transport and deposition are related to seasonal variations in atmospheric circulation (Knippertz and Todd, 2012). The intertropical convergence zone (ITCZ) shifts meridionally from ~12 °N during boreal winter to ~ 21 °N during boreal summer resulting in a seasonal change in rainfall and winds over the African continent (Nicholson, 2009).

During summer, continental rainfall is most intense and the rain belt is positioned near ~10°N with smaller amounts of rainfall near ~ 21°N. Dust emission is driven by low level jets, so-called 'haboobs', African easterly waves (AEWs) and high surface winds associated with the Saharan heat low (Knippertz and Todd, 2012). N trade winds blow in coastal Mauritania year-round (National Geospatial-Intelligence Agency, 2006). The offshore transport of Saharan dust particles occurs within the 'Saharan air layer' (SAL) at an altitude of about 3 km (Prospero and Carlson, 1970;Carlson and Prospero, 1972;Prospero and Carlson, 1972;Diaz et al., 1976).

During winter, dust emission is driven by the break-down of nocturnal low-level jets after sunrise, increased surges in Harmattan winds and microscale dust devils and dust plumes (Koch and Renno, 2005;Knippertz and Todd,

Atmos. Chem. Phys. Discuss., doi:10.5194/acp-2017-131, 2017
Manuscript under review for journal Atmos. Chem. Phys.
Discussion started: 16 February 2017

Atmospheric Chemistry and Physics Discussions

2012). Dust is transported within the low-level NE and E trade winds to coastal Mauritania (Dobson, 1781) and also offshore to the sediment-trap mooring sites (Stuut et al., 2005).

1.4 Oceanic setting

The surface-water circulation offshore Cape Blanc is influenced by the southward-flowing Canary Current (CC) and the poleward-flowing coastal counter current or Mauritania Current (Fig. 1). Underneath, the undercurrent is flowing poleward in water depths down to 1000 m (Fig. 1). The undercurrent flows along the continental slope and transports water masses originating from ~5-10 °N to latitudes up to 26 °N. The poleward flowing South Atlantic Central Water (SACW) and the southward flowing North Atlantic Central Water (NACW) are situated below the counter current and meet offshore Cape Blanc (Mittelstaedt, 1991). The study area is positioned in a zone of permanent annual upwelling of sub-surface water masses (Cropper et al., 2014). The NACW and SACW may be upwelled and mixed laterally off Cape Blanc (Meunier et al., 2012). The permanent annual upwelling of nutrient-rich subsurface waters results in high phytoplankton concentrations offshore Cape Blanc (Van Camp et al., 1991). As a result, the surface waters are rich in organic detritus, usually referred to as 'marine snow', and faecal pellets which are produced by marine zooplankton (Iversen et al., 2010).

Individual Saharan dust particles which settle at the ocean surface hardly settle to the deep sea. Instead, fine dust particles can be transferred from the ocean surface to the deep sea by being incorporated into marine snow aggregates and faecal pellets (Ternon et al., 2010). The aggregate formation and ballasting of marine snow aggregates and faecal pellets with marine carbonate and opal as well as with Saharan dust particles results in anomalously high sinking velocities (Ploug et al., 2008b;Fischer and Karakas, 2009;Iversen et al., 2010;Iversen and Ploug, 2010;Iversen and Robert, 2015). Dust-loaded particles that sink into the deeper water column are assumed to have a mean settling speed of ~ 240 m d^{-1} at site CB (Fischer and Karakas, 2009).

The buoy Carmen (~21°15' N, ~20°56' W) and the sediment trap mooring sites CB (~21°16' N, ~20°48' W) and CBi (~20°45' N, ~18°42' W) are located ~ 200 and ~ 80 nautical miles offshore Cape Blanc in the north-eastern (NE) equatorial Atlantic ocean (Fig. 1).

Atmos. Chem. Phys. Discuss., doi:10.5194/acp-2017-131, 2017
Manuscript under review for journal Atmos. Chem. Phys.
Discussion started: 16 February 2017

Atmospheric Chemistry and Physics Discussions

2. Material and Methods

2.1 Sediment traps

Saharan dust was collected in the ocean using marine sediment traps of the type Kiel (model SMT-234/243) which are conical with an opening of 0.5 m^2 (Fig. 2). The principle of particle collection is much the same as described by Van der Does et al. (2016b) and Korte et al. (2016). At the top of the opening a honeycomb grid is installed to prevent large swimmers (>1 cm) from entering the trap. The sediment traps were equipped with twenty sample cups which rotated according to a pre-programmed sampling interval (Fischer and Wefer, 1991). The sampling interval was chosen depending on the timing of the ship expeditions.

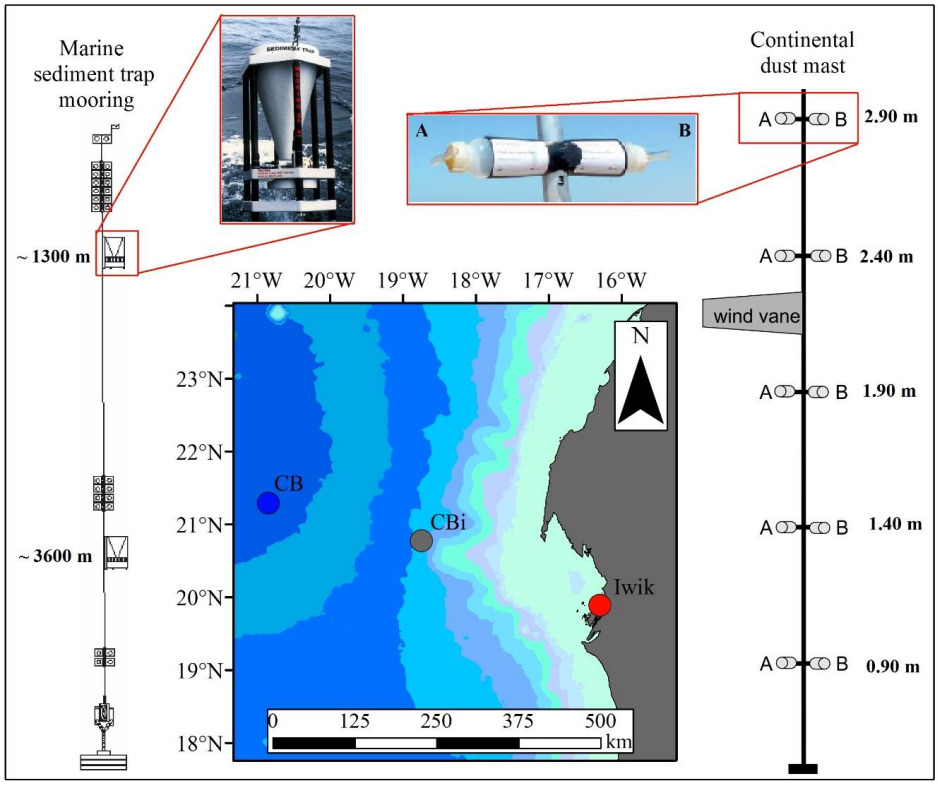

Figure 2: The marine sediment trap moorings CB and CBi offshore Cape Blanc and the dust masts near Iwik, Mauritania. On the left, a sketch of the sediment trap mooring (sketch of CB 24 copied from Fischer et al. (2013)) together with a photograph of the trap (downloaded from www.kum-kiel.de) is displayed. On the right, a sketch of the dust mast together with a photograph of the MWAC sampling bottles is depicted.

The sampling intervals were synchronized between the two sites. The intervals ranged from 9.5 days to 21.5 days (Table 1). Deployment and recovery of the sediment-trap samples was performed during the Research Vessel Poseidon expeditions POS445 (Fischer et al., 2013), POS464 (Fischer et al., 2014) and POS481 (Fischer et al., 2015a) (Table 1). The working steps related to the trap deployment and treatment are described in Fischer and Wefer (1991). In order to prevent outflow of water from the cups during sampling, each sampling cup was filled

Atmos. Chem. Phys. Discuss., doi:10.5194/acp-2017-131, 2017
Manuscript under review for journal Atmos. Chem. Phys.
Discussion started: 16 February 2017

Atmospheric Chemistry and Physics Discussions

with 20 ml of filtered (<0.2 µm) seawater with a salinity of 40 ‰. To produce seawater with a salinity of 40 ‰, 100 g NaCl suprapur was added to 1 l of filtered seawater. Microbial and zooplankton activity was inhibited inside the trap samples by adding 1 ml of a saturated solution of the biocide $HgCl_2$ per 100 ml of seawater. After recovery, swimmers <1 cm were removed from the samples by sieving each sample through a 1 mm mesh. A McLane rotary liquid splitter was used to split the <1 mm fraction of each sample into five equal aliquots.

The samples of two sediment-trap deployments during 2013-2015 of the sediment trap mooring stations CB and CBi were chosen for grain-size analyses (Table 1). The upper traps sampled at an average water depth of ~ 1300 m and the lower trap sampled at a water depth of ~3600 m (Table 1). Dust which settles at the ocean surface is advected by ocean currents during settling in the water column. As a result, particles that settle in an area of ~ 40 x 40 km^2 in the ocean surface above the traps may be collected in a water depth of ~ 1300 m (Friese et al., 2016). Two winter and two summer samples were chosen for X-ray Diffraction (XRD) measurements (Table 2).

Table 1: Specifications of the sediment trap samples collected during 2013-2015 chosen for flux and grain-size analysis.

Trap series	Trap type	Sampling period	Cruise deployment	Cruise recovery	Position	Trap depth [m]	Water depth [m]	No. of samples	Sampling intervals
CBi 11 upper (GeoB 18006-2)	SMT 243	29.01.2013 – 25.03.2014	Pos445	Pos464	20°46.4' N 18°44.4' W	1406	2800	18	17x21d, 1 x20d
CBi 12 upper (GeoB 19402-01)	SMT 234 NE	14.02.2014 - 23.02.2015	Pos464	Pos481	20°46.4' N 18°44.5' W	1356	2750	20	1x12.5 d, 19x19.5
CB 24 upper (GeoB 18001-1)	SMT 234 NE	24.01.2013 - 05.02.2014	Pos445	Pos464	21°16.9' N 20°50.6' W	1214	4160	18	1x26 d, 16x21 d, 1x15 d
CB 25 lower (GeoB 19401-1)	SMT 234 NE	07.02.2014 – 21.02.2015	Pos464	Pos481	21°17.8' N 20°47.8' W	3622	4160	20	19x19.5 d, 1x9.5 d

Table 2: Sediment trap and MWAC samples chosen for mineralogical investigation.

Sample	Sampling period	Mast	Bottle	Elevation/water depth [m]	Sampling interval
CBi 11 upper # 8	25.06.-16.07.13	-	-	1406	21d
CBi 12 upper # 2	26.02.-18.03.14	-	-	1356	20d
CBi 12 upper # 10	01.08.-21.08.14	-	-	1356	20d
CBi 12 upper # 17	16.12.-04.01.15	-	-	1356	19d
Iwik 13-7-2-3B	24.06.-15.07.13	2	B	1.90	21d
Iwik 14-8-2-5B	15.08.-15.09.14	2	B	2.90	31d
Iwik 14-12-1-4A	15.12.14-18.01.15	1	A	2.40	34d
Iwik 14-2-2-5B	15.02.-15.03.14	2	B	2.90	28d

Atmos. Chem. Phys. Discuss., doi:10.5194/acp-2017-131, 2017
Manuscript under review for journal Atmos. Chem. Phys.
Discussion started: 16 February 2017

Atmospheric Chemistry and Physics Discussions

2.2 Modified Wilson and Cooke (MWAC) samplers

Saharan dust was collected on land near Iwik, Mauritania, with a passive dust sampler consisting of two masts (1 and 2) with two sets of five air sampling bottles each (A and B, Fig. 2). The dust sampling bottles are referred to as modified Wilson and Cooke (MWAC) samplers (Wilson and Cooke, 1980;Mendez et al., 2011) and consist of a closed Polyethylene bottle through which the wind can pass via two glass tubes of 8 mm openings. Thus, a big difference between the traps and the MWAC collectors is the much smaller collection area of the MWAC collectors with 44 mm^2. The MWAC dust sampler was chosen because it is one of the most common (Zobeck et al., 2003) and most efficient dust samplers (Goossens and Offer, 2000). The sampling bottles were mounted horizontally at five different heights. The masts were aligned to the ambient wind direction via a wind vane (Fig. 2).

The samples collected in 2013-2015 were chosen for subsequent flux and grain-size analyses (Table 3). Saltating dust particles may be collected in the lower sampling bottles at 90 cm. However, the aim was to analyse dust transported in suspension to enable a better comparison between the continental and marine sites. Therefore, the highest sampling bottles attached to the mast at 2.90 m height were used for microscope, flux and grain-size analysis (Table 2). One series of bottles (series B2) of mast 2 were analysed with the microscope. The other three replicate samples (bottles A1 and B1 of mast 1, bottles A2 of mast 2) were analysed for flux and grain-size analysis. Out of the three replicate samples, the sample with the highest mass was chosen for the interpretation of the flux and grain-size data because this bottle was assumed to have sampled most efficiently. Three samples mounted at a height of 2.40 m of mast 2 were chosen to test the effect of the chemical pre-treatments that we do to isolate the terrigenous fraction from marine sediments on the resulting grain-size distributions (Fig. 2). Two winter and two summer samples that contained enough material were chosen for XRD measurements (Table 2).

Furthermore, dust was sampled with a MWAC dust sampler mounted on the mast of buoy Carmen, at about 2 m above the sea surface (Stuut et al., 2015). A wind vane was attached to the mast which aligned the sampler to the ambient wind direction. This MWAC dust sample was also analysed for grain-size distribution.

Table 3: Specifications of the MWAC samples collected during 2013-2015 chosen for flux and grain-size analysis.

Dust collector series	Trap type	Sampling period	Position	Height [m]	No. of samples	Sampling intervals
Iwik 13	MWAC	27.01.2013 – 20.01.2014	19°53.1' N 16° 17.6' W	2.90	11	19 d, 28 d. 32 d, 29 d, 40 d, 21 d, 31 d, 61 d, 31 d, 31 d, 35 d
Iwik 14	MWAC	20.01.2014 - 18.01.2015	19°53.1' N 16° 17.6' W	2.90	13	26 d,. 28 d, 31 d, 30 d, 31 d, 30 d, 31 d, 31 d, 30 d, 32 d, 29 d, 34 d
CB-MWAC	MWAC	23.08.2014 – 16.11.2015	21°15.8' N 20°56.1' W	2.00	1	450 d

2.3 Microscopy

The MWAC samples chosen for microscopic investigation were analysed with a Leica M165 C microscope. Microscope pictures were taken using a Leica DFC420 camera attached to the microscope. The software Leica application suite 3.8 was used for taking the pictures.

Atmos. Chem. Phys. Discuss., doi:10.5194/acp-2017-131, 2017
Manuscript under review for journal Atmos. Chem. Phys.
Discussion started: 16 February 2017

Atmospheric Chemistry and Physics Discussions

2.4 Dust and lithogenic fluxes

1/5 splits of the sediment trap samples were analysed for dust fluxes and the bulk components following the method presented in Fischer and Wefer (1991). The lithogenic flux [$mgm^{-2}d^{-1}$] was estimated according to Eq. (1):

$$lithogenic\ material = dust = total\ mass - carbonate - opal - 2\ x\ Corg \quad (1)$$

Organic carbon was measured after the removal of carbonate with 2N HCl using a CHN-Analyser (HERAEUS). Total carbon was estimated by combustion without pre-treatment. Carbonate was determined according to Eq. (2):

$$carbonate = total\ carbon - organic\ carbon \quad (2)$$

Biogenic opal was determined with a sequential leaching technique (Müller and Schneider, 1993).
The MWAC samples chosen for dust flux analyses were weighed on a Mettler-Toledo AT261 Delta Range balance with a precision of 0.0001 g. Mean atmospheric dust concentrations were estimated as Eq. (3):

$$\mathrm{DL} = \frac{MAR}{(v*A)} * \frac{1}{\eta} \quad (3)$$

Where DL is the mean dust concentration [μgm^{-3}], MAR is the mass accumulation rate [μgs^{-1}], v is the mean wind speed per sampling month [ms^{-1}], A is the cross-sectional area of the inlet tube of the MWAC sampler [m^2] and η is the estimated sampling efficiency of MWAC bottles. A sampling efficiency of 90 % was assumed based on an efficiency study of Goossens and Offer (2000). Mean horizontal dust fluxes were calculated according to Eq. (4):

$$F_h = \frac{MAR}{A} * \frac{1}{\eta} \quad (4)$$

where F_h is the horizontal dust flux [$mgm^{-2}d^{-1}$], MAR is the mass accumulation rate [mgd^{-1}], A is the cross-sectional area of the inlet tube of the MWAC sampler [m^2] and η is the estimated sampling efficiency of MWAC bottles.

2.5 Particle size

A 1/25 split of the marine sediment trap samples was analysed for particle size of the terrigenous fraction. The samples were pre-treated before measurement in order to isolate this fraction (see also Filipsson et al. (2011);Friese et al. (2016), Meyer et al. (2013) and Stuut (2001) for methodology) with the following steps: (1) removal of organic matter: Addition of 10 ml of H_2O_2 (35%) to the sediment sample and subsequent boiling until the reaction stops, (2) removal of calcium carbonate: Addition of 10 ml HCl (10%) to the sediment sample and subsequent boiling for exactly 1 minute and (3) removal of biogenic silica: Adding 6 g of NaOH pellets to the sediment sample and subsequent boiling for 10 minutes. Before particle-size analysis, 10 drops of $Na_4P_2O_7*10H_2O$ were added to each sample to assure the full disaggregation of the particles. The pre-treatment of the MWAC samples differed from the pre-treatment of the sediment trap samples as, obviously, these samples did not contain any biogenic material originating from marine plankton. Further, the disaggregation of particles needed to be kept at minimum to allow for the study of dust transport processes, the so-called 'minimally dispersed' aeolian fraction (McTainsh et al., 1997). Therefore, the MWAC samples were solely pre-treated with three drops of $Na_4P_2O_7*10H_2O$ before analysis. The marine sediment-trap samples as well as the MWAC samples were analysed with the laser particle sizer Beckmann Coulter LS13320 at NIOZ using a Micro Liquid Module (MLM). This instrument allows quick,

Atmos. Chem. Phys. Discuss., doi:10.5194/acp-2017-131, 2017
Manuscript under review for journal Atmos. Chem. Phys.
Discussion started: 16 February 2017

Atmospheric Chemistry and Physics Discussions

accurate, and precise data acquisition of large size intervals (Bloemsma et al., 2012). An analytical error of ± 1.26 µm (± 4.00 %) was considered for the measurements (Friese et al., 2016).

To investigate the comparability of the MWAC samples with the oceanic sediment-trap samples, the particle-size distribution of the MWAC sample attached to buoy Carmen was compared to the averaged particle-size distributions of the upper and lower trap series at site CB (Fig. 3a). The grain-size distribution of the MWAC sample was comparable to both sediment trap time series even though the sampling time period was different. To ensure that the pre-treatment steps of the traps did not influence the terrigenous fraction itself, tests were made in which the on-land MWAC samples were exposed to the same pre-treatment steps as the marine samples (Fig. 3b). One spring sample has been measured with and without a chemical pre-treatment. Two fall dust samples were obtained from the same height and mast and sampling interval, however from different bottles (A and B) and were measured with and without pre-treatment. The figure indicates that a pre-treatment of the Iwik dust samples did not alter the particle distributions of the samples significantly. Further, the particle-size distribution of dust sampled with different bottles is comparable.

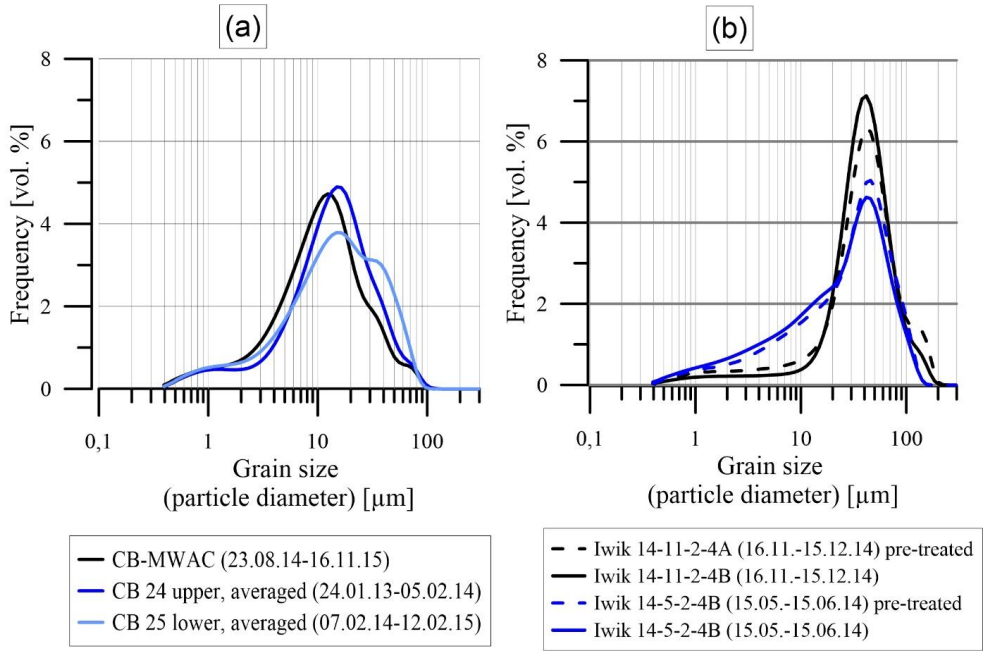

Figure 3: (a) Grain-size distributions for the station CB: Dust sampled with the MWAC sampler 2 m above sea level, with the upper sediment trap at 1214 mbsl and the lower trap at 3622 mbsl. (b) Grain-size distributions of samples of the Iwik 14 time series which have been pre-treated with HCl, H_2O_2 and NaOH (dotted lines) and without pre-treatment (lines).

2.5 Mineral assemblages

Two winter and two summer samples of the MWAC dust collector and the sediment-trap series CBi were chosen for XRD analysis (Table 3). X-Ray Diffraction pattern analyses were carried out in the laboratory of the research

group Crystallography (University of Bremen, Central Laboratory for Crystallography and Applied Material Sciences, ZEKAM, Dept. of Geosciences).

Due to the small amount of material in the available dust samples (< 100 mg), the preparation for the measurement was done by pipetting a demi-water-sample mixture on glass slides. A thorough preparation commonly increases reproducibility of the results, however, the standard deviation given by Moore and Reynolds (1989) of ±5% can be considered as a general guideline for mineral groups with >20% clay fraction. In addition, the determination of well-crystallized minerals like quartz, calcite or aragonite can be done with better standard deviations (Tucker and Tucker, 1988;Vogt et al., 2002). The X- Ray Diffraction was measured on a Philips X'Pert Pro multipurpose diffractometer equipped with a Cu-tube (k_α 1.541, 45 kV, 40 mA), a fixed divergence slit of ¼°, a secondary Ni-Filter and the X'Celerator detector system. The measurements were carried out as a continuous scan from 3 – 85° 2θ, with a calculated step size of 0.016° 2θ (calculated time per step was 100 seconds). Mineral identification was accomplished using the Philips software X'Pert HighScore™, which, besides the mineral identification, can give a semi-quantitative value for each identified mineral on the basis of Relative Intensity Ratio (R.I.R.)-values. The R.I.R.-values are calculated as the ratio of the intensity of the most intense reflex of a specific mineral phase to the intensity of the most intense reflex of pure corundum (I/Ic) referring to the "matrix-flushing method" after Chung (1974). Unfortunately R.I.R. values are sparse for clay minerals and long chain organic materials hampered the quantification of our samples.

2.6 Meteorological data

The obtained flux and size data were compared to near-by meteorological data (wind speed, wind direction and precipitation).

Wind direction, wind speed and precipitation data with a 20 minute resolution were gathered for the sampling site CB (21°17' N – 21°12' N, 20°56' W - 20°54' W) during the buoy Carmen deployments from November 2013 to September 2015 with a Vaisala WXT520 meteorology sensor. The size of the dataset was reduced by calculating four hour averages. Moreover, wind direction and wind-speed data with a resolution of five minutes to one hour were gathered during sampling at site Iwik (19°53.1' N, 16° 17.6' W) from January 2013 to January 2015 with a Davis 6250 Vantage Vue meteorology sensor. The size of the dataset was reduced by calculating one-hour averages. Further hourly precipitation data were gathered from the station Arkeiss (20° 7' N, -16° 15' W) from December 2013 to March 2015 with another Davis 6250 Vantage Vue meteorology sensor. Continental hourly wind direction and wind-speed data was acquired for the Nouadhibou meteorological station (20° 55' N, 17° 1' W) online from the Cedar Lake Ventures website (https://weatherspark.com).

Local daily precipitation data (TRMM 3B42 dataset, 0.25° spatial resolution) were derived from the Giovanni online data system, developed and maintained by the NASA GES DISC (http://gdata1.sci.gsfc.nasa.gov). Daily precipitation data were downloaded as area-averages around CBi (20° 58' N - 20° 34' N, 18° 56 W - 18° 32' W), Iwik (19° 41' N - 20° 5'N, 16° 29' W - 16° 05' W), CB/Carmen (21° 05' N - 21° 29' N, 21° 02' W - 20° 38' W) and Arkeiss (20° 19' N - 19° 55' N, 16° 28' W - 16° 04' W) according to the assumed catchment area of the upper trap (~ 40 x 40 km^2).

337
338 **2.7 Mapping with ArcMap**

339 The mapping software ArcMap version 10.3.1 was used to analyze the source regions of the dust samples
340 investigated for mineralogical composition. A map was created with four-day back-trajectories for days with a
341 dust-storm event as depicted on satellite images. In addition, the African surface lithology was included in the map
342 and soils rich in the minerals calcite, kaolinite and chlorite were marked.

343 Satellite quasi-true colour RGB images (MODIS dataset) were retrieved from the NASA Ocean Biology
344 Distributed Active Archive Centre (*OB.DAAC*), Goddard Space Flight Centre, Greenbelt MD, on their website
345 (http://oceancolor.gsfc.nasa.gov).

346 Four-day back trajectories (at altitudes of 10, 3000, 4500 and 5500m) were calculated ending at the dust collector
347 site Iwik (19°52' N, 16°17' W) and at the proximal marine trap site CBi (20°46',18°44' W) using the Hybrid
348 Single Particle Langrangian Integrated Trajectory (HYSPLIT) model (Stein et al., 2015) and the reanalysis dataset
349 (2.5° spatial resolution) on the NOAA website at http://ready.arl.noaa.gov.

350 An ArcGIS layer file of the African surface lithology
351 (new_af_lithology_w_glbcvr_waterbdy_90m_dd84_final.lyr) was downloaded from the U.S. Geological survey
352 (USGS) website: http://rmgsc.cr.usgs.gov/outgoing/ecosystems/AfricaData.

353 An ArcGIS shape file of the African soils (DSMW.shp) was downloaded from the website of the food and
354 agriculture organization of the United Nations (FAO) at
355 http://www.fao.org/geonetwork/srv/en/metadata.show?id=14116. The mean percentage of calcite, chlorite and
356 kaolinite in the clay fraction of Saharan soils in general and for each soil type is given by Journet et al. (2014).
357 The average percentages of calcite, chlorite and kaolinite in the clay fraction of Saharan soils are 8.9 %, 4.1 % and
358 29 %, respectively (Journet et al., 2014). Soils with larger percentages of calcite, chlorite or kaolinite in the clay
359 fraction than the average percentages were marked in the ArcGIS map.

360
361
362
363
364
365
366
367
368
369
370

Atmos. Chem. Phys. Discuss., doi:10.5194/acp-2017-131, 2017
Manuscript under review for journal Atmos. Chem. Phys.
Discussion started: 16 February 2017

Atmospheric Chemistry and Physics Discussions

3. Results

3.1 Meteorology

In Fig. 4 the meteorological data of the sites Carmen/CB, CBi, Iwik, Arkeiss and Nouadhibou during 2013 to 2014 are presented (see Fig 4a for location of the sites). The rainfall frequency is given in Fig. 4b for each site. The number of rainfall events were calculated regarding the TRMM stations for precipitation rates >1 mmd^{-1} because smaller precipitation amounts which were detected by the satellite may not actually reach the ground. Regarding the ground stations Carmen and Arkeiss, a threshold of >0.2 mmd^{-1} was used in order to exclude events which may be related to anomalously high moisture instead of rainfall.

According to the TRMM satellite product the annual precipitation frequency was larger on the shoreline (station Arkeiss and Iwik) than offshore (station CBi and Carmen) (Fig. 4b). This may be explained by a decrease in atmospheric water vapor content due to precipitation when the winds move westward. Moreover, the TRMM satellite product indicated larger rainfall frequencies during the summer season compared to the winter season regarding the oceanic stations Carmen, CBi, Iwik and Arkeiss. Larger summer rainfall frequencies can be explained by the summer northward shift of the ITCZ to ~ 21° N resulting in more frequent moist convection and rainfall in the study area.

The annual rainfall frequency at the site Arkeiss and the summer rainfall frequencies at the sites Arkeiss and Carmen compare quite well between the sensors and the TRMM observations. However, the spatial and seasonal trends observed by the TRMM data were not supported by the sensor on buoy Carmen and by the ground station in Arkeiss. The larger annual and winter rainfall frequency recorded with the sensor on buoy Carmen may be related to water emission from the ocean surface during time periods with strong surface winds. Further, disagreements between the ground stations and the TRMM stations maybe caused by the local signal recorded by the respective rain sensor. A larger number of rain sensors would most likely improve the comparability to the TRMM data.

Atmos. Chem. Phys. Discuss., doi:10.5194/acp-2017-131, 2017
Manuscript under review for journal Atmos. Chem. Phys.
Discussion started: 16 February 2017

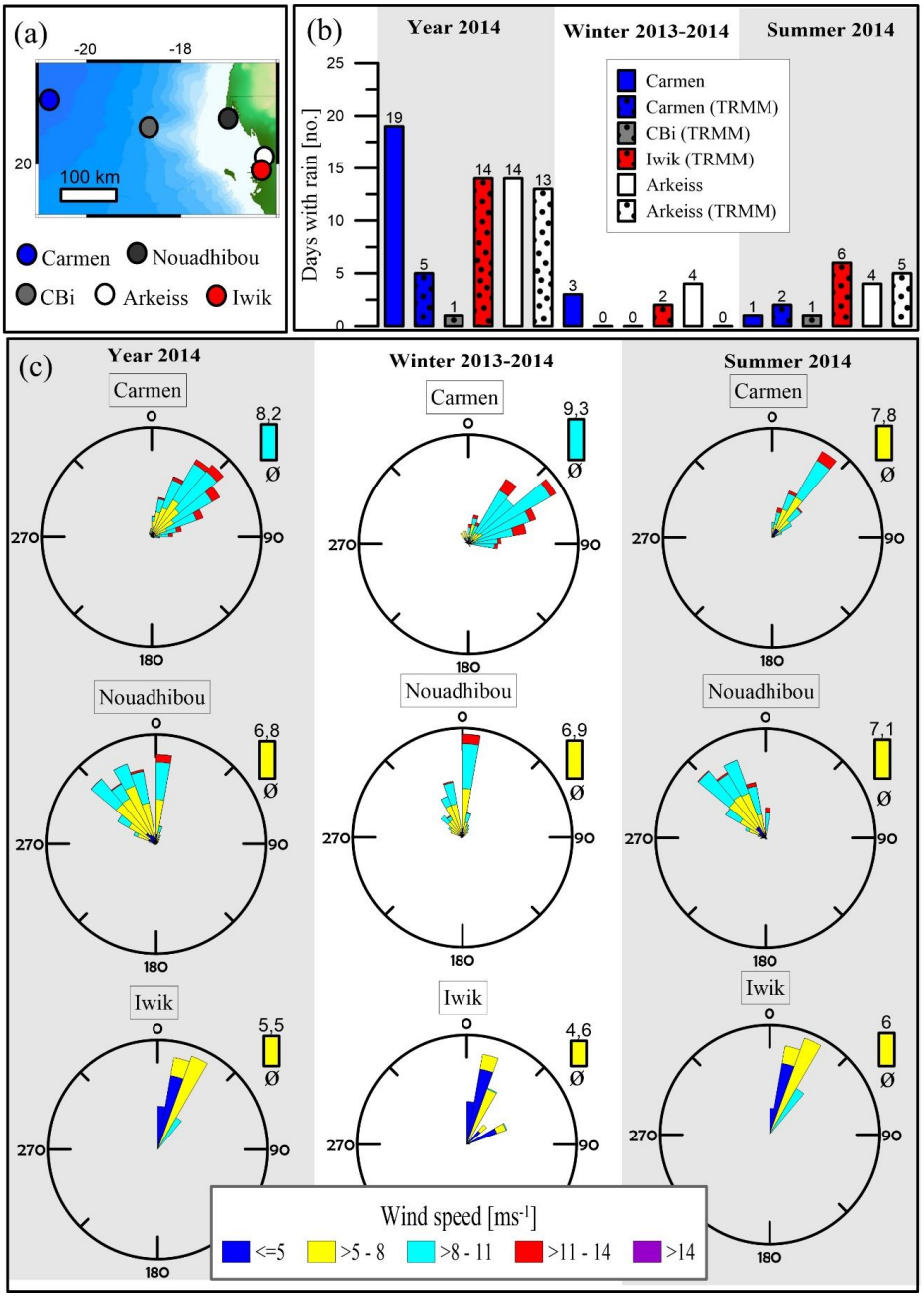

394

395 **Figure 4: Meteorological data (a) map showing the study sites CB, CBi and Iwik and the meteorological station in**
396 **Nouadhibou under investigation (b) precipitation at the study sites CB, CBi and Iwik (c) wind direction and speed at**
397 **the study sites CB and Iwik and at the meteorological station in Nouadhibou.**

398 The wind direction and speed for the ground stations Carmen, Nouadhibou and Iwik are displayed in Fig. 4c. The
399 annual average surface wind velocity was maximum offshore at buoy site Carmen/CB with ~ 8 m/s. The buoy

Atmos. Chem. Phys. Discuss., doi:10.5194/acp-2017-131, 2017
Manuscript under review for journal Atmos. Chem. Phys.
Discussion started: 16 February 2017

Atmospheric Chemistry and Physics Discussions

recorded a larger average wind velocity during winter than during summer, which is consistent with this season being dominated by the Trades. On the shoreline, the average wind velocity was slightly larger during summer than during winter. The predominant annual wind direction was NE at site Carmen and Iwik, while predominant NW winds were recorded for the site Nouadhibou. The wind direction changed from predominant NE during winter to predominant NNE direction during summer at site Carmen. A similar, but less pronounced seasonal trend can be observed for the continental site Iwik. In Nouadhibou, the predominant winter wind direction is NNW switching to a predominant NW wind direction during summer. Obviously, with winds originating from the open ocean, not a lot of dust is anticipated. Therefore, we interpret these wind directions as being very local and caused by the shape of the peninsula of Cape Blanc.

3. 2 Microscope findings of the dust samples from Iwik

In Fig. 5 the results of the microscopy investigation of the Iwik 2013 time series are presented. In general, the majority of the particles consisted of angular and moderately spherical quartz grains with a diameter of ~ 50 µm (Fig. 5a,b). A small percentage of large platy minerals with a diameter of ~ 200 µm were found in all samples (Fig. 5b). Large quartz grains with a diameter of ~ 150 to 200 µm were detected in 45 % of the samples. An anomalously high percentage of sub-angular and moderately spherical quartz grains with an average diameter of ~ 200 µm was observed in one summer sample (Fig. 5c). Aggregated grains occurred in all samples. However, the percentage and size of the aggregates as well as the size of the aggregated grains differed from sample to sample. Usually, the size of the aggregated grains was ~ 50 µm (Fig. 5a). Two samples were characterized by aggregates composed of particles with a smaller size of ~ 20 µm (Fig. 5d).

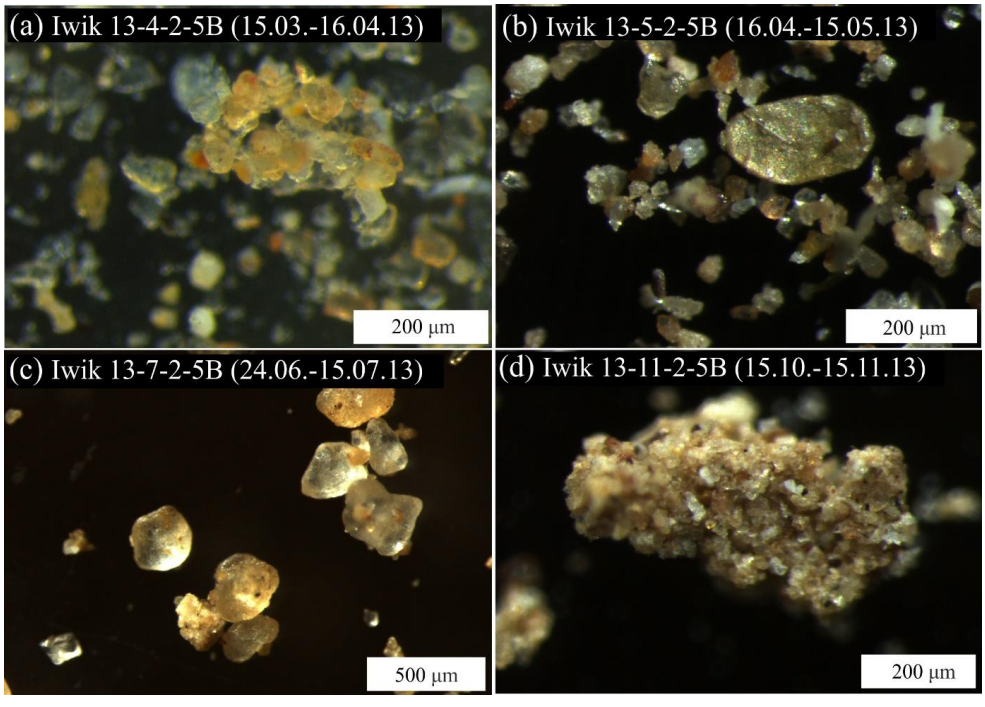

Atmos. Chem. Phys. Discuss., doi:10.5194/acp-2017-131, 2017
Manuscript under review for journal Atmos. Chem. Phys.
Discussion started: 16 February 2017

Atmospheric Chemistry and Physics Discussions

Figure 5: Microscopic photographs of selected dust samples from the Iwik 2013 time series. (a) Spring dust sample with a ~ 250 x 150 µm aggregate, (b) spring dust sample with a ~ 200 x 100 µm mica chip, (c) summer dust sample with ~ 200 x 200 µm quartz grains, (d) fall dust sample with a ~ 600 x 250 µm aggregate.

3.3 Dust fluxes and size on land and in the ocean

In Table 4 the average dust fluxes are given for the sampling sites Iwik, CBi and CB. The dust concentrations at site Iwik were determined based on the measured wind speed of the meteorological sensor attached to the sampling mast. For four samples no wind data were available due to a failure of the instrument. For these samples a wind velocity was assumed based on the seasonal averages calculated from the available wind data of the meteorology sensor in Iwik (Fig. 4c). The annual average horizontal dust fluxes at site Iwik were of the same order of magnitude during 2013 and 2014. The PM_{10} concentration was calculated in order to enable a comparison to other study sites where only dust particles smaller than 10 µm were sampled. The annual average dust fluxes decreased from the on-land site Iwik towards the proximal site CBi and the distal site CB. The dust fluxes were about 1000 times smaller at the oceanic sites compared to the continental site. A stronger decrease in the fluxes was observed from site Iwik to CB during summer compared to winter. The variation in the seasonal average dust fluxes were well comparable between the continental and oceanic site CBi. A seasonal trend in the dust fluxes could not be observed for the ocean sites CBi and CB. However, a seasonal trend was observed for site Iwik when taking into account the spring and fall samples. The average dust concentration was maximum during spring plus winter 2013 and 2014 with 393 μgm^{-3} and 341 μgm^{-3}, respectively, and minimum in fall 2013 and 2014 with 48 and 68 μgm^{-3}, respectively. The dust fluxes generally decreased with collection height in the mast between 90 and 290 cm (not shown).

Table 4: Seasonal and annual average dust fluxes and average modal grain size, mean/mode ratio and standard deviation of the grain-size distributions from Iwik 13-14, CBi 11-12 upper and CB 24 upper time-series.

Series	Year	Winter	Summer	Annual
Average dust fluxes [mg.m^{-2}.d^{-1}] (dust concentration [µg.m^{-3}])				
Iwik 13	2013	10000 (30)	113000 (268)	95000 (214)
CBi 11 upper	2013	106	168	99
CB 24 upper	2013	53	44	45
Iwik14	2014	208000 (603)	55000 (127)	102000 (275)
CBi 11+12 upper	2014	98	20	47
Average modal grain size [µm]				
Iwik 13	2013	44	49	48
CBi 11 upper	2013	27	39	29
CB 24 upper	2013	16	17	16
Iwik 14	2014	45	49	48
CBi 11+12 upper	2014	34	44	33
Average mean/mode ratio [µm]				
Iwik 13	2013	0.7	0.6	0.6
CBi 11 upper	2013	0.5	0.3	0.5
CB 24 upper	2013	0.7	0.8	0.7
Iwik14	2014	0.6	0.4	0.6
CBi 11+12 upper	2014	0.5	0.3	0.5
Average standard deviation [µm]				
Iwik 13	2013	2.8	3.1	3.0
CBi 11 upper	2013	3.0	3.3	3.1
CB 24 upper	2013	2.7	2.6	2.6
Iwik 14	2014	2.8	3.5	3.1
CBi 11+12 upper	2014	3.1	3.3	3.0

Atmos. Chem. Phys. Discuss., doi:10.5194/acp-2017-131, 2017
Manuscript under review for journal Atmos. Chem. Phys.
Discussion started: 16 February 2017

Atmospheric Chemistry and Physics Discussions

442

443 The statistical values of the measured grain-size distributions for the stations CB, CBi and Iwik are given in Table
444 4. In addition, the measured grain-size distributions for the time series of the stations CB, CBi and Iwik are
445 displayed in Fig. 6. In Fig. 6a the average grain-size distribution for the samples of each of the three stations for
446 the year 2013 are given. The maximum measured particle size decreased from ~223 µm on land at site Iwik to
447 ~169 µm at the proximal site CBi and ~140 µm at the distal site CB (Fig. 6a). In addition, the average modal grain
448 size decreased from ~48 µm at site Iwik to 16 µm at site CB (Table 4). Bimodal grain-size distributions were
449 encountered for 23 % of the CBi 11-12 samples, 13 % of the Iwik 13-14 samples, and none of the CB 24 samples.
450 The bimodal distributions of the Iwik 13-14 time series were characterized by an additional fine mode peaking at
451 ~16 µm besides the more pronounced and variable coarse mode peaking at ~42 to 55 µm. Two of the Iwik dust
452 samples characterized by a fine grain-size peak were collected during summer and fall respectively. The sorting
453 of the CB samples was better than the sorting of the Iwik and CBi time series as indicated by the average geometric
454 standard deviations of 2.6 µm for CB and 3.1 µm for both Iwik and CBi (Table 4). The lowest average mean/mode
455 ratio was recorded for the CBi time-series with ~0.5 due to the weak sorting of the samples (Table 4).

456 In Fig. 6b-c the measured grain-size distributions for winter and summer samples are displayed. The averaged
457 modal grain size for the summer samples was coarser grained compared to the winter samples of the respective
458 grain-size time series (Table 4). The seasonality in modal grain size was largest for the CBi 11 upper trap series
459 of the year 2013 with a difference of ~12 µm (Table 4). The average standard deviation was larger and the average
460 mean/mode ratio was smaller in the summer samples compared to the winter samples regarding the sites Iwik and
461 CBi (Table 4). In other words: the summer samples of sites CBi and Iwik were less well sorted (Fig. 6b and c).
462 This seasonal trend was not observed in the CB 24 upper samples which were generally well sorted. (Table 4).

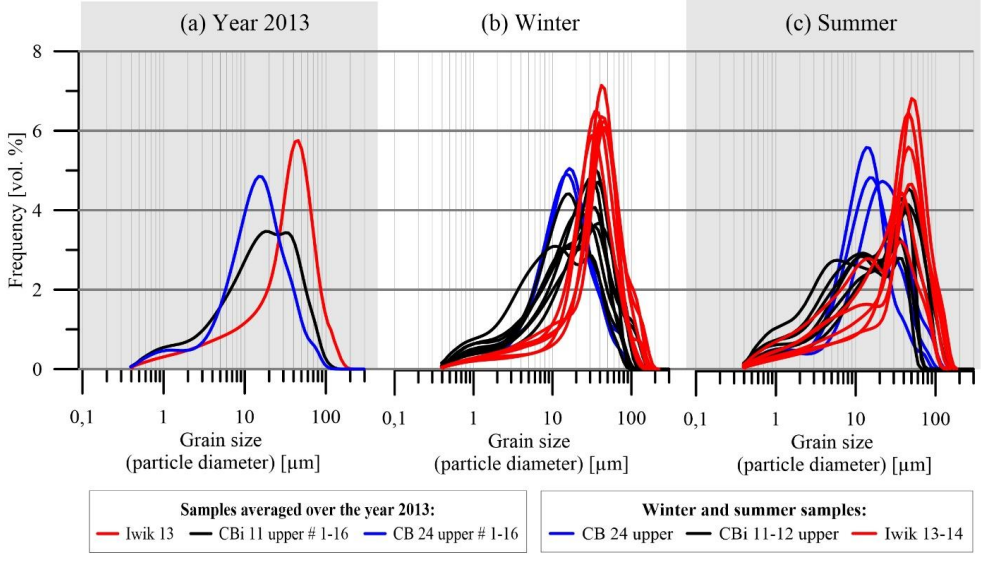

463

464 **Figure 6: Grain-size distributions of the stations Iwik, CBi and CB (a) averaged for the samples of the year 2013 (b)**
465 **winter samples (c) summer samples.**

Atmos. Chem. Phys. Discuss., doi:10.5194/acp-2017-131, 2017
Manuscript under review for journal Atmos. Chem. Phys.
Discussion started: 16 February 2017

Atmospheric Chemistry and Physics Discussions

In Fig. 7a –c the results of the correlation between the characteristics of the dust sampled on land and the local meteorological data are presented. In Fig. 7a the particle sizes were correlated to the surface wind speed data (N = 13 samples). A correlation above a coefficient of determination (R^2) of 0.3 was considered significant at the 95 % confidence level for two-tailed probabilities. The modal particle size of the Iwik samples showed a positive linear correlation with the daily wind speed events with $R^2 = 0.5$, which is significant at the 99.31 % confidence level. A better positive linear correlation was obtained when excluding the spring sample resulting in $R^2 = 0.7$ which is significant at the 99.96 % confidence level.

In Fig. 7b the dust fluxes were correlated to the surface wind-speed data (N = 10 samples). A correlation above $R^2 = 0.4$ was considered significant at the 95 % confidence level for two-tailed probabilities. The horizontal dust flux of the Iwik samples correlated positively to the daily wind speed events during the sampling interval with $R^2 = 0.7$ which is significant at the 99.75 % confidence level. Moreover, a significant linear correlation with $R^2 = 0.6$ was observed at the 99.15 % confidence level between the dust fluxes and the mean wind strengths during the sampling intervals (not shown).

In Fig.7c the particle size of the Iwik summer samples was correlated to the local TRMM precipitation data (N= 6 samples). In this case a correlation above $R^2 = 0.7$ was considered significant at the 95 % confidence level for two-tailed probabilities. A good linear negative correlation with $R^2 = 0.9$ was observed which is significant at the 99.78 % confidence level.

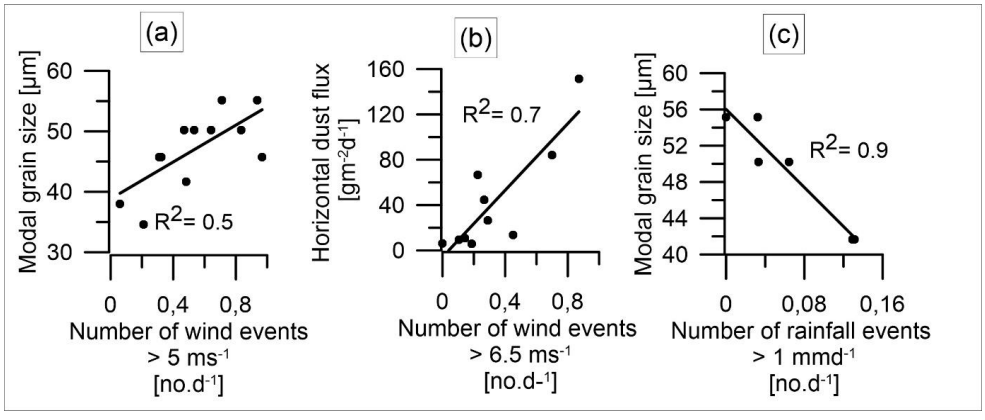

Figure 7: Correlation between the observed local surface wind speed at site Iwik and the measured (a) modal grain size and (b) flux. (c) Correlation between the observed local precipitation at site Iwik (TRMM data) and the modal grain size of the summer samples.

3.4 Mineral assemblage of dust sampled on land and in the ocean

In Table 5 the mineralogical composition averaged over all eight samples, averaged over the four Iwik samples and the four CBi samples is given. All dust samples contained the minerals quartz and mica. Further minerals that occurred with significant quantities but which were not present in all dust samples were feldspar, amphibole, zeolite, chlorite and palygorskite. Calcite, dolomite, gibbsite, kaolinite, smectite, sepiolite, fluellite, anhydrite, rutile and serpentine occurred only in some samples resulting in a low average abundance ≤ 1%. However, we argue that these minerals can be used as dust source indicators because of (1) the characteristic distribution of

494 gibbsite, kaolinite, smectite and sepiolite in North Africa according to different weathering regimes (Biscaye,
495 1964) and (2) the characteristic occurrence of fluellite, anhydrite, rutile and serpentine according to outcropping
496 rock type (Deer et al., 1992). Further minerals that occur in low abundances (≤ 3%) were summarized as 'other
497 minerals' and will not be discussed in the manuscript. While the continental samples were dominated by quartz
498 and feldspar, the marine samples were dominated by mica, followed by quartz and feldspar.

499 **Table 5: Results of the mineralogical investigation: Mineral assemblage averaged over all samples (Total), the Iwik**
500 **samples (Iwik) and the CBi samples (CBi).**

*	Qz [%]	Fsp [%]	Mi [%]	Amf [%]	Pal [%]	Chl [%]	Cc [%]	Dol [%]	Gib [%]	Zeo [%]	Kao [%]	Sme [%]	Se [%]	Rut [%]	Serp [%]	Ga [%]	Anh [%]	Flu [%]
Total	25.1	21.5	25.5	5.1	3.4	4.4	0.6	0.1	1.0	3.8	0.9	0.4	1.1	0.5	0.3	0.1	0.1	1.1
Iwik	33.3	30.8	18.0	5.0	3.3	1.8	1.3	0.3	2.0	0.0	0.0	0.0	0.0	0.8	0.5	0.0	0.0	0.0
CBi	17.0	12.3	33.0	5.3	3.5	7.0	0.0	0.0	0.0	7.5	1.8	0.8	2.3	0.3	0.0	0.3	0.3	2.3

*Qz = quartz, Fsp = feldspar, Mi = mica, Amf = amphibole, Pal = palygorsite, Chl = chlorite, Cc = calcite, Dol = dolomite, Gib = gibbsite, Zeo = zeolite, Kao = kaolinite, Sme = smectite, Se = sepiolite, Rut = rutile, Serp = serpentine, Ga = garnet, Anh = anhydrite, Flu = fluellite

501

502 In Fig. 8a-c the results of the mineralogical investigation of the eight chosen dust samples are presented. Figure 8a
503 depicts again the average composition of the samples per sampling site (N=4). The minerals zeolite, anhydrite,
504 garnet, sepiolite, fluellite, kaolinite and smectite were only found in the marine samples. Only the continental
505 sample of 15.08.-15.09.14 contained traces of zeolite. While gibbsite, serpentine, calcite and dolomite were
506 detected in the continental dust samples, these minerals were absent in all marine samples. The absence of calcite
507 and gibbsite may have been caused by the pre-treatment of the marine sediment-trap samples with HCl. Although
508 the concentration of the used acid is fairly low (10%) and the exposure time of the samples was exactly 1 minute,
509 we cannot exclude that carbonate minerals were dissolved. Therefore, the absence of these minerals in the marine
510 traps will not be discussed further.

511 In the following, the seasonality in the average mineralogical composition will be outlined for each site as given
512 in Fig. 8b,c. At site Iwik, the winter dust samples were characterized by the occurrence of chlorite, serpentine and
513 rutile, while the summer samples were characterized by the minerals gibbsite and dolomite. At site CBi, the winter
514 dust samples were characterized by the occurrence of the minerals sepiolite, fluellite, kaolinite, smectite, garnet
515 and anhydrite, while the summer samples were characterized by the mineral rutile. Only for the marine trap
516 samples an annual average chlorite/kaolinite ratio (C/K = 4) could be derived owing to the occurrence of kaolinite.

Atmos. Chem. Phys. Discuss., doi:10.5194/acp-2017-131, 2017
Manuscript under review for journal Atmos. Chem. Phys.
Discussion started: 16 February 2017

Atmospheric Chemistry and Physics Discussions

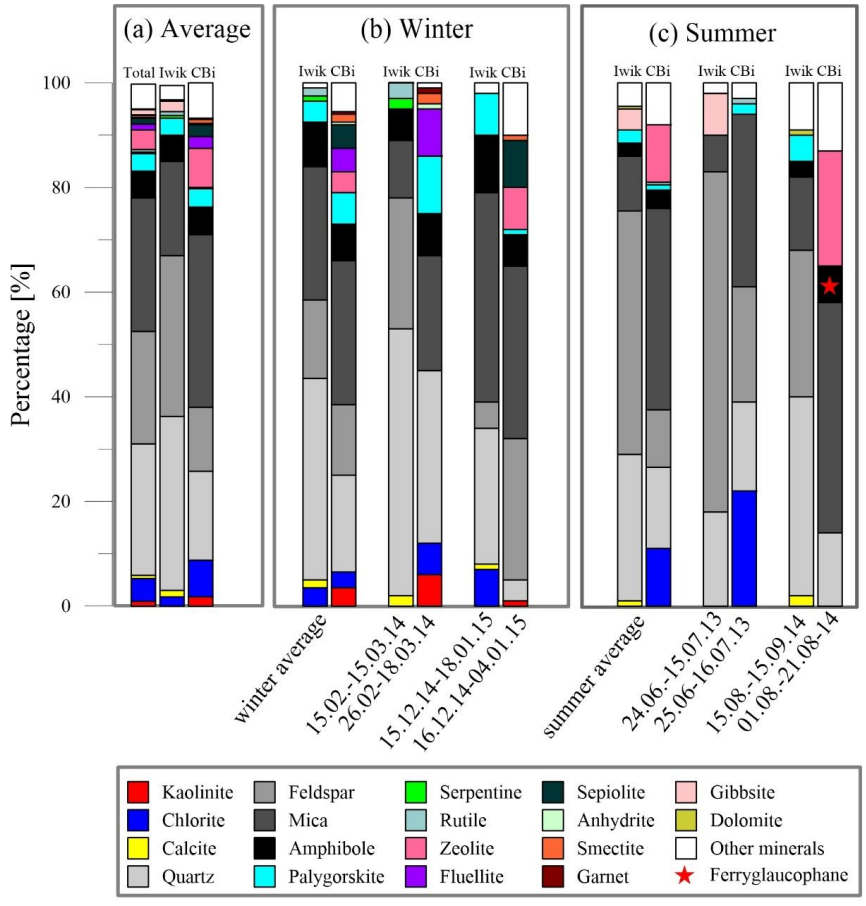

Figure 8: Mineralogical composition (a) averaged over all samples and for sites Iwik and CBi, (b) averaged for the winter samples at sites Iwik and CBi and for each individual winter sample and (c) averaged for the summer samples at sites Iwik and CBi and for each individual summer sample. The category 'other minerals' comprises the minerals todorokite, sodalite, konicklite, guyanaite, nitratnine, urea, bernalite, akermanite, mixed-layer clay and talc.

3.5 Identification of dust source regions using ArcMap

In Fig. 9-12 the results of the four day back-trajectory analysis are presented for each sample which has been analyzed for mineralogical composition. Two heights, 10 m (according to Stuut et al. (2005)) and 4500 m (according to Skonieczny et al. (2013)) were chosen to cover both low- (trades) and high-level (SAL) dust transport. Only the low-level back-trajectories were plotted for site Iwik because of the correlation of the measured dust characteristics to the low-level wind speed. Moreover, the MWAC samplers were designed to only sample dry deposition, whereas the marine sampling sites collect material settling through the water column, i.e., dust resulting from both dry- and wet deposition. The back-trajectories at 3000 and 5500 m can be found in the supplements.

Figure 9 illustrates a typical late-winter situation. During the sampling interval at least two dust storms occurred (Fig. 9c,d). Both the low-level back-trajectories ending at the continental trap site Iwik and at the oceanic trap site

Atmos. Chem. Phys. Discuss., doi:10.5194/acp-2017-131, 2017
Manuscript under review for journal Atmos. Chem. Phys.
Discussion started: 16 February 2017

Atmospheric Chemistry and Physics Discussions

CBi point to a dust source within the major **PSA 2** (Scheuvens et al., 2013). Some calcite was present in the continental dust sample, but no chlorite nor kaolinite was detected. Therefore, the dust source was most likely located in the nearby southwestern Reguibat Shield where sediments are rich in calcite and quartz and depleted in chlorite and kaolinite (Fig. 9a). Dust deposited in the marine traps during the time interval was characterized by the occurrence of chlorite and kaolinite. A small area of chlorite-rich sediments is located in the shoreline of the Western Sahara (Fig. 9b). However, kaolinite is not present in anomalously high amounts in the proposed source area (Fig. 9b).

Atmos. Chem. Phys. Discuss., doi:10.5194/acp-2017-131, 2017
Manuscript under review for journal Atmos. Chem. Phys.
Discussion started: 16 February 2017

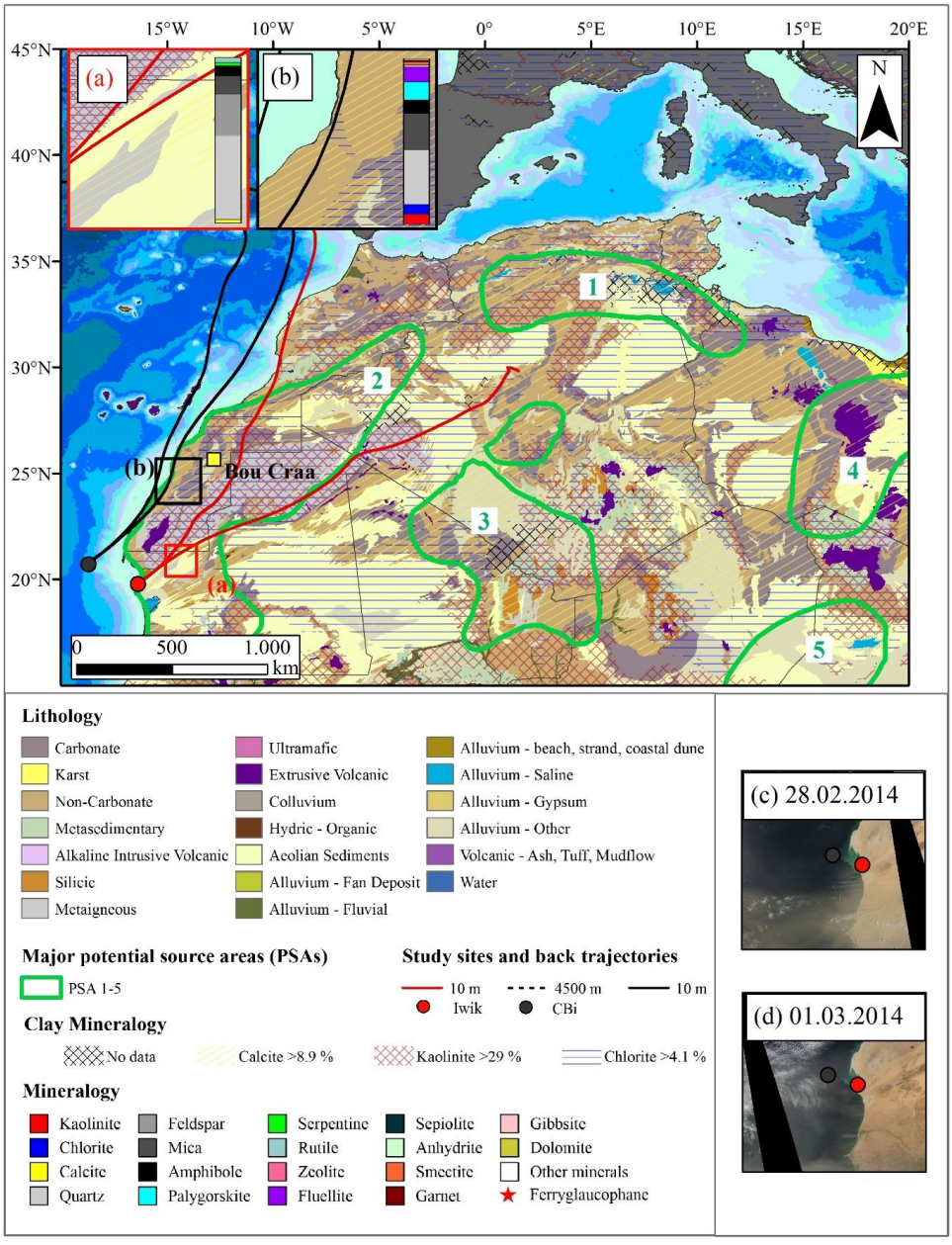

Figure 9: Low-level (10 m) four-day back trajectories of dust events ending during the sampling interval 15.02.-15.03.14 at site Iwik and during the sampling interval 26.02.-18.03.14 at site CBi. The potential dust source areas and the mineralogy of the samples are given in the subfigures a-b. The dust-storm events occurring during the sampling interval are indicated in subfigures c-d.

Figure 10 represents a typical early-winter situation. During the sampling interval at least three dust storms occurred (Fig. 10e-g) and one lasted for several days which complicates the determination of the likely dust source

Atmos. Chem. Phys. Discuss., doi:10.5194/acp-2017-131, 2017
Manuscript under review for journal Atmos. Chem. Phys.
Discussion started: 16 February 2017

Atmospheric Chemistry and Physics Discussions

areas. All back trajectories pass through the major **PSA 2** and some point to the **PSA 1** and **PSA 3** (Scheuvens et al., 2013). Dust sampled in the marine traps during this sampling interval did not contain any chlorite, while the dust trapped at Iwik did. Chlorite may have been supplied to Iwik from a source area nearby the Senegal-Mauritania Basin (Fig. 10a) or as far as the eastern Taoudeni Basin (Fig. 10b) due to the anomalously high chlorite content of the soils in these areas. The continental sample is further characterized by the occurrence of calcite and the absence of kaolinite which fits to the soils of the chosen source areas (Fig. 10a,b). The marine sample was characterized by the occurrence of zeolite and absence of chlorite. Therefore, zeolite may have been derived from the extrusive volcanic rocks of the northern Taoudeni Basin (Fig. 10c). A further source area might be the southern shoreline of Western Sahara similar to what was observed for the sample obtained during winter 2014 (Fig. 9b, Fig. 10d). Again, the marine winter sample contained the mineral kaolinite which cannot be explained with the back-trajectories and the soil map.

Atmos. Chem. Phys. Discuss., doi:10.5194/acp-2017-131, 2017
Manuscript under review for journal Atmos. Chem. Phys.
Discussion started: 16 February 2017

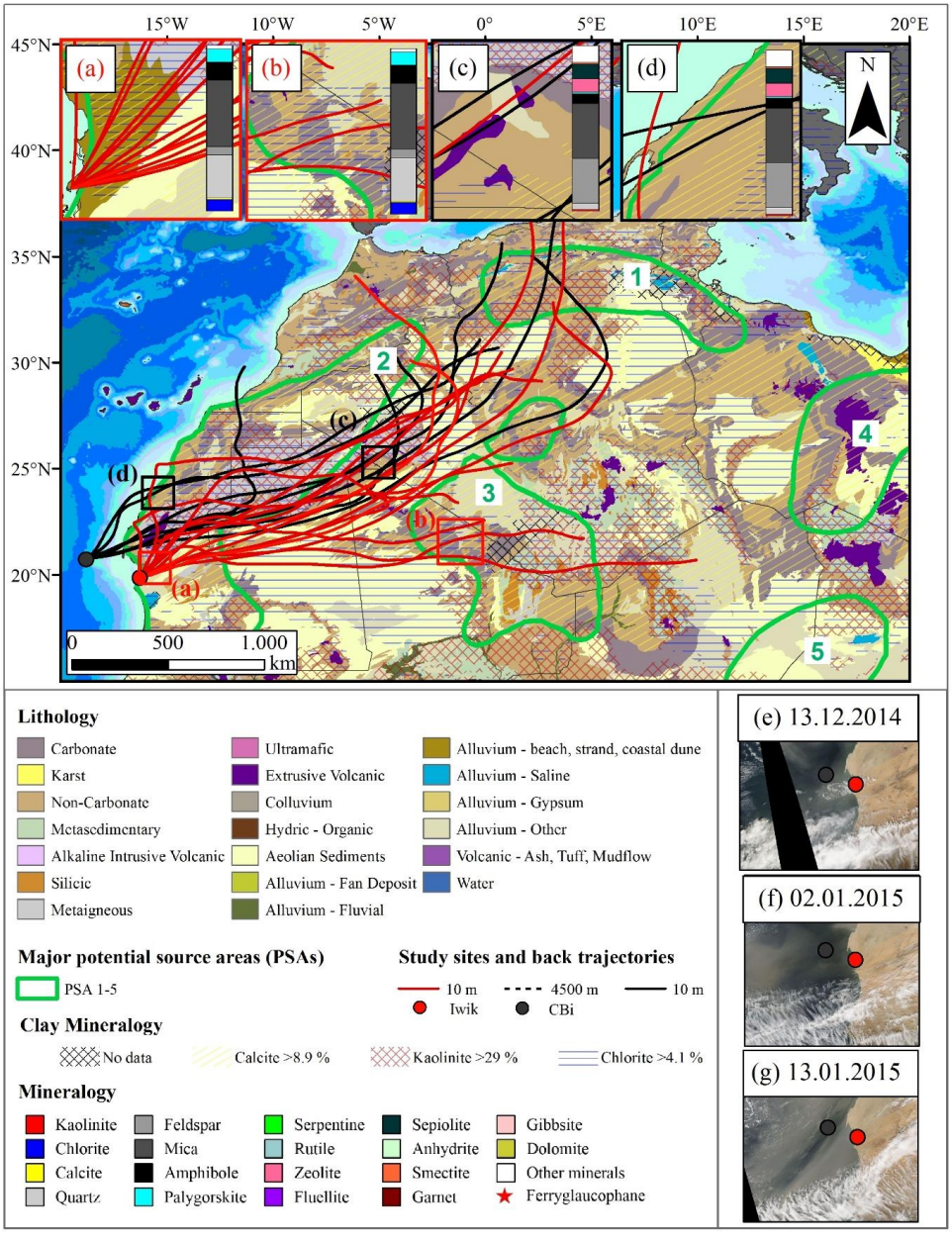

Figure 10: Low-level (10 m) four-day back trajectories of dust events ending during the sampling interval 15.12.14-18.01.15 at site Iwik and during the sampling interval 16.12.14-04.01.15 at site CBi. The potential source areas and the mineralogy of the samples are given in the subfigures a-c. The dust storm events occurring during the sampling interval are indicated in subfigures e-g.

In Fig. 11 a typical early-summer situation is presented. Only one dust storm event was observed during the sampling interval (Fig. 11c). The low-level back trajectories ending at site CBi run offshore. The low-level back

Atmos. Chem. Phys. Discuss., doi:10.5194/acp-2017-131, 2017
Manuscript under review for journal Atmos. Chem. Phys.
Discussion started: 16 February 2017

566 trajectory ending at site Iwik passes through the major **PSA 2** and the high-level back trajectory passes through
567 the major **PSA 2** and **3** (Scheuvens et al., 2013). Dust sampled on land at site Iwik was characterized by the absence
568 of chlorite, kaolinite and calcite which fits to the soils of northern Tidra Island (Fig. 11a). In contrast, dust sampled
569 offshore at site CBi was characterized by chlorite and by the absence of kaolinite which fits to the chlorite rich
570 soils in the Mauritanides of Mauritania (Fig. 11b).

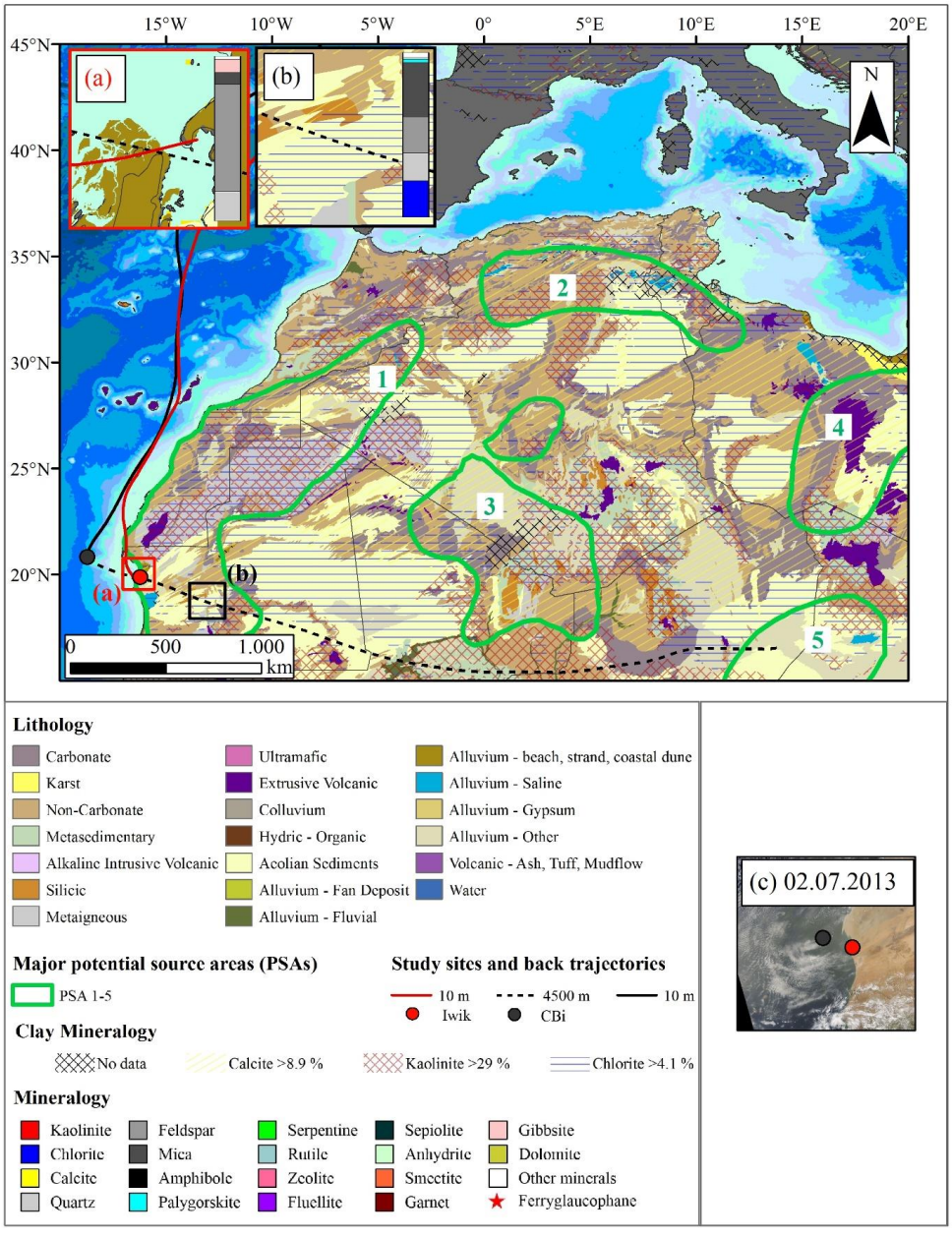

571

Atmos. Chem. Phys. Discuss., doi:10.5194/acp-2017-131, 2017
Manuscript under review for journal Atmos. Chem. Phys.
Discussion started: 16 February 2017

Atmospheric Chemistry and Physics Discussions

572 **Figure 11: High- (4500 m) and low-level (10 m) four-day back trajectories of a dust event ending during the sampling**
573 **interval 24.06.-15.07.13 at site Iwik and during the sampling interval 25.06.-16.07.13 at site CBi. The potential source**
574 **areas and the mineralogy of the samples are given in the subfigures a-b. The dust storm event is indicated in subfigure**
575 **c.**

576 In Fig. 12 a typical late-summer situation is illustrated. At least five separate dust events could be identified (Fig.
577 12f-j) of which one lasted for two days. The low-level back trajectories ending at site CBi run offshore. The low-
578 level back trajectories ending at site Iwik pass through the major **PSA 2**. The high-level back trajectories pass
579 through the major **PSA 2**, **PSA3** and **PSA 4** (Scheuvens et al., 2013). Dust deposited in the continental traps was
580 characterized by the presence of calcite and the absence of chlorite and kaolinite. Therefore, the source area of the
581 dust was most likely in the Western Sahara where soils rich in calcite but poor in chlorite and kaolinite are located
582 (Fig. 12a,b). Dust sampled with the oceanic traps during this sampling interval was characterized by the absence
583 of chlorite and kaolinite and by the presence of a high percentage of zeolite (22 %) (Fig. 8c). Therefore, a possible
584 source area may have been extrusive volcanic rocks of the northern Taoudeni Basin (Fig. 12c) and the Fezzan
585 uplift (Fig. 12e). Ferryglaucophane may have been sourced by the Pharusian belt (Fig. 12d).

Atmos. Chem. Phys. Discuss., doi:10.5194/acp-2017-131, 2017
Manuscript under review for journal Atmos. Chem. Phys.
Discussion started: 16 February 2017

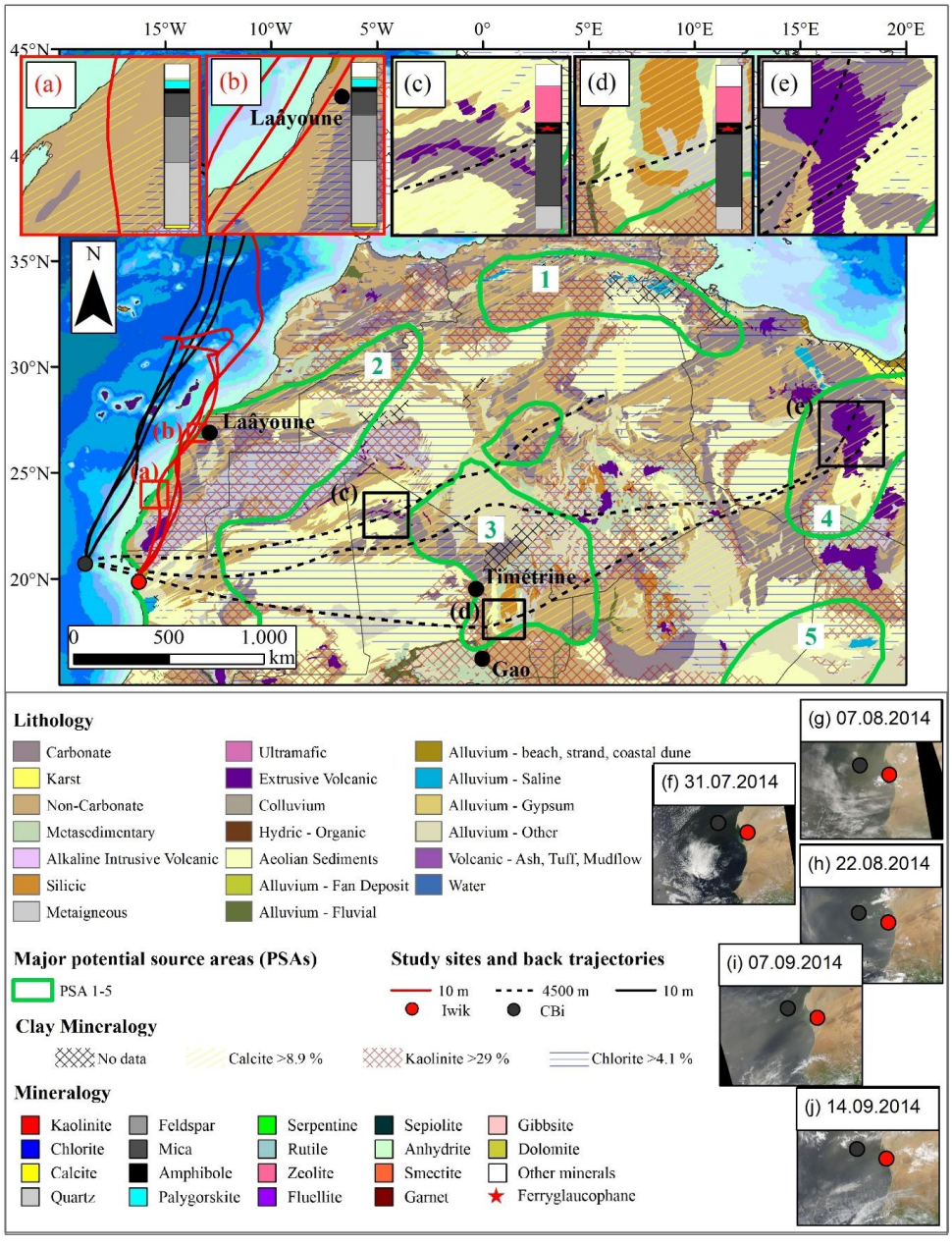

Figure 12: High- (4500 m) and low-level (10 m) four-day back trajectories of dust events ending during the sampling interval 15.08.-15.09.14 at site Iwik and during the sampling interval 01.08.-21.08.14 at site CBi. The potential source areas and the mineralogy of the samples are given in the subfigures a-c. The dust storm events are indicated in subfigures e-i.

Atmos. Chem. Phys. Discuss., doi:10.5194/acp-2017-131, 2017
Manuscript under review for journal Atmos. Chem. Phys.
Discussion started: 16 February 2017

Atmospheric Chemistry and Physics Discussions

4. Discussion

4.1 Comparison of dust collected on land and in the ocean

4.1.1 Dust concentrations

Annual average dust concentrations of ~214 (2013) and 275 μgm^{-3} (2014) were estimated for the site Iwik (Table 4). These estimates were larger than what has been measured for background dust concentrations in Morocco which were in the order of 100 μgm^{-3} during spring 2006 (Kandler et al., 2009). However, in Morocco dust was collected at a larger height of 4 m and the sampling time is much shorter leading to the monitoring of less dust events. The horizontal dust fluxes at site Iwik correlated positively to wind speed (Fig. 7b) and decreased with collection height (not shown). This underscores the proximity of this continental site to the dust emission source.

At the distal oceanic site CB, the annual average dust deposition flux was ~ 45 $mgm^{-2}d^{-1}$ (Table 4). The dust flux was slightly larger than the average annual dust flux observed at site CB between 1988 and 2012 with ~ 30 $mgm^{-2}d^{-1}$ (Fischer et al., 2015b). The slightly larger dust fluxes may have been caused by the anomalously high frequency in dust storm events as observed on satellite images occurring during the studied time period (not shown). The average horizontal fluxes at site Iwik were ~ 1000 times larger with ~ 100000 $mgm^{-2}d^{-1}$ (Table 4) due to the different sampling technique. The MWAC samplers do not measure deposition fluxes but foremost dust concentrations. Only 1% or less drops out of a moving dust cloud, hence, the horizontal dust flux is at least ~100 times higher than the dust deposition flux (Goossens, 2008). In addition, the observed general decrease in the dust flux from the site Iwik to the sites CBi and CB can be explained via the increase in the distance to the source area. Decreased dust deposition fluxes offshore NW Africa with increasing distance from the African coast were also observed by Bory and Newton (2000) analysing the lithogenic fluxes in marine sediment traps. The stronger decrease in the dust fluxes from site Iwik to CB during summer compared to winter (Table 4) may be explained in the following. During summer, dust was additionally transported with the trades to the site Iwik, (Fig. 9-12) leading to anomalously higher dust deposition at site Iwik compared to the oceanic sites. Further, the washout of dust during offshore transport may have depleted the atmospheric dust cloud resulting in strongly decreased dust deposition fluxes at site CB compared to site CBi during summer.

4.1.2 Dust transport

The measured grain-size distributions for dust trapped at 2.90 m on land at site Iwik and for dust settling in the ocean were nearly all unimodal (Fig. 6). Unimodal grain-size distributions are typical for wind-blown sediments (Pye, 1995). Unimodal grain-size distributions were also measured for dust deposited in a vertical dust sampler in M'Bour (Skonieczny et al., 2011), dust sampled on ship vessels (Stuut et al., 2005) and in other sediment trap samples offshore NW Africa (Ratmeyer et al., 1999b;Friese et al., 2016;Van der Does et al., 2016a).

The measured annual average modal grain size at site Iwik was 48 µm (Table 4). The obtained average annual modal grain size was close to the coarse mode of 44 µm observed by Gillies et al. (1996) for dust trapped at a height of 10 m during spring in Fakarbé (Mali) which is located about 700 km southeast of Iwik. Gillies et al. (1996) conclude that the coarse mode in the dust samples points to locally-derived dust. Based on this observation, we argue that also the dust trapped near Iwik was most likely generally of regional instead of long-distance provenance. The distance to the main source area may be, however, not in the direct surrounding of the dust collector since dust sampled with MWAC samplers in the vicinity of barchan dunes of the Bodélé depression at

631 2.4 m height is characterized by a larger modal particle size of ~ 100 µm (Chappell et al., 2008). The annual
632 average modal and maximum particle size gradually decreased from the on-land site Iwik, to the proximal oceanic
633 site CBi and the distal oceanic site CB (Table 4, Fig. 6a). This decrease in particle size between the stations CB
634 and CBi was observed before and was attributed to the preferred gravitational settling of coarse particles during
635 dust transport (Friese et al., 2016). Moreover, many studies have confirmed a downwind fining of the terrigenous
636 fraction of surface sediments offshore NW Africa (Radczewski, 1939;Lange, 1975;Fütterer, 1980;Koopmann,
637 1981;Holz et al., 2004), and it is intuitively logical.

638 The three samples of the Iwik time series that were characterized by an additional small peak in the grain-size
639 distribution around ~ 16 µm were sampled during sampling intervals of anomalously high wind velocity. The back-
640 trajectories of one of these samples pointed towards a proximal and more distal dust source (Fig. 12a,b). Therefore,
641 it may be possible that wind velocities were high enough during the sampling interval to transport dust from more
642 distant sources (Fig. 12b) to the sampling site resulting in the small peak in the grain-size distributions. On the
643 other hand, microscopic examination prior to particle-size analyses of the Iwik samples revealed that the samples
644 included many aggregates (Fig. 5d). Hence, locally derived aggregates may have been sampled during periods of
645 high wind velocities. These aggregates may have been dispersed in the demineralized water during the
646 measurement of the laser resulting in the observed additional fine peak at ~16 µm. Further, precipitation was
647 encountered according to the TRMM data during the sampling interval of two of these three samples. Therefore,
648 a further explanation for the bimodal grain-size distributions may be the deposition of finer dust particles from
649 higher altitude of the SAL due to precipitation. Two of the three oceanic samples that were characterized by
650 bimodal grain-size distributions have several proposed dust source areas each (Fig. 10, 12). Thus, the sampling of
651 long- as well as short-travelled dust may have resulted in a bimodal grain-size distribution.

652 At the on-land site Iwik, a positive correlation between the modal grain sizes and wind velocities was observed
653 (Fig. 7a). This implied that dust was transported with the trade winds from sources of a quite constant distance
654 year-round. During dust storm events particles with a diameter of 40 to 50 µm may be transported ~ 100 km (Tsoar
655 and Pye, 1987). The proposed source areas all fall in this range except for the winter sample of 2014-2015 (Fig.
656 10). The winter sample was characterized by an anomalously low modal grain size of 38 µm and particles of this
657 size may be transported more than 100 km during dust storm events (Tsoar and Pye, 1987). Moreover, Van der
658 Does et al. (2016a) observed how particles up to 100 µm were transported ~ 3500 km across the Atlantic Ocean.

659 **4.1.3 Dust mineralogical composition**

660 In the dust sampled at Iwik the minerals quartz, feldspar, mica, amphibole, palygorskite, chlorite, calcite, dolomite,
661 gibbsite, rutile and serpentine were present (Fig. 8a). The observed occurrence of the minerals quartz, feldspar,
662 mica, chlorite and calcite has also been described for the bulk size fraction of soil samples and dust samples
663 collected in Mauritania (Schütz and Sebert, 1987). Palygorskite, mica and chlorite have also been detected by
664 Skonieczny et al. (2013) in the PM_{30} size fraction of a three-year time series of dust deposition at M'Bour, Senegal,
665 more than 500km south of Iwik, Mauritania. Smectite and kaolinite, which were absent in the Iwik samples, were
666 the dominant minerals of the dust sampled at M'Bour (Skonieczny et al., 2013). Smectite and kaolinite are
667 considered as indicative for wet tropical soils and their relative abundance in soils increases southwards along the
668 northwest African coast (Biscaye, 1964;Lange, 1982). We argue that the mineralogical differences between the
669 two sites are explained by the >500 km distance between Iwik and M'Bour and the fact that the latter station is

surrounded by tropical soils. Gibbsite, rutile and serpentine have not been reported in any continental dust study so far and thus seem to be indicative for locally-derived dust (Fig. 9a, Fig. 11a).

The dust sampled at the proximal marine site CBi contained the minerals quartz, feldspar, mica, amphibole, palygorskite, chlorite, zeolite, kaolinite, smectite, sepiolite, rutile, garnet, anhydrite and fluellite (Fig. 8a). The first seven of these minerals were also found in the clay and/or silt and sand fraction of Saharan dust sampled during ship cruises parallel to the coast about 70 km off Cape Blanc (Chester et al., 1971) and perpendicular to the coast about 80 to 180 km off Cape Blanc (Chester and Johnson, 1971a). Analogous to the samples of this study, the PM_{20} fraction of surface sediments of the piston cores RC05-57, RC05-60 and A180-44 also feature zeolites and the surface sediments of core RCRC05-57 also traces of pyrophyllite (sepiolite belongs to the pyrophyllite group) (Biscaye, 1964). Further, rutile was also present in the silt and sand fraction of Saharan dust sampled perpendicular to the coast on the research vessel (Chester and Johnson, 1971a). Palygorskite was found in the clay fraction of the surface sediment of sediment core GIK12329 (19° 22' N, 19°56' W) offshore Cape Blanc and is considered a characteristic mineral of Saharan dust (Lange, 1975). The observed annual average C/K ratio (C/K=4) recorded for the bulk size fraction of the trap samples was larger than the C/K ratio (C/K=0.3-1) recorded in the clay fraction of surface sediment samples offshore Cape Blanc by Lange (1982). The disagreement may be due to the generally larger percentage of kaolinite in the clay fraction compared to the silt fraction (Journet et al., 2014).

The dust samples of the site Iwik were further characterized by a dominance in quartz and feldspar (Fig. 8a). A dominance in quartz has also been described for continental dust samples and soil samples collected in Mauritania by Schütz and Sebert (1987). More than 20 papers published XRD data of northern African dust reporting quartz as the main mineral in most dust samples (Scheuvens et al., 2013). Moreover, the continental sampling site is surrounded by sand dunes which are rich in quartz minerals (Schlüter, 2008;Lancaster, 2013). A high quartz content may therefore point to predominantly locally derived dust. The observed increase in micas and decrease in quartz and feldspar observed for the marine samples relative to the Iwik samples (Fig. 8a) can be explained via the preferential gravitational settling of the larger dust minerals quartz and feldspar during transport (Delany et al., 1967;Chester and Johnson, 1971a;Glaccum and Prospero, 1980;Schütz and Sebert, 1987). A strong downwind decrease in quartz content in Saharan dust was also observed by Korte et al. (2016).

4.2 Mineralogy as a provenancing tool

4.2.1 Dust collected on land

The back trajectories indicate that the dust sources for the dust collected in Iwik during winter were located NE and E of the sampling site (Fig. 9a, Fig.10a,b), while those during summer were located W (within the PNBA) and NNE of the sampling site (Fig. 11a, Fig. 12a,b). This is in accordance with a change in the dominant local surface wind direction from NE in winter to NNE in summer (Fig. 2) and is also reflected in the clay-mineralogical composition of the samples.

Generally, there is not much variability in the clay-mineralogical composition of the Iwik samples. The back trajectories for the winter sample of 2014 indicate that the material was blown from the southwestern Reguibat Shield (**PSA 2)** (Fig. 9a). The lack of palygorskite in this sample does not fit to the proposed bulk palygorskite content (1-30 %) of **PSA 2** (Scheuvens et al., 2013). We argue that the sampled dust was most likely derived from

a single localized source instead of externally mixed sources of **PSA 2** during transport. The sample included the characteristic minerals rutile and serpentine (Fig. 8b) which are usually a result of metamorphic processes (Deer et al., 1992). Indeed, the western Reguibat Shield is composed of metamorphic and granitic rocks (Schofield et al. (2006) and references therein) and the rocks are intruded by serpentinites (Schlüter, 2008). The sample was further characterized by the highest quartz percentage among all samples (~ 50 %) (Fig. 8b). The sand dunes of the Azefal sand sea which cover part of the southwestern Reguibat Shield might have sourced these quartz grains (Fig. 9a). The sand dunes may have been fed by outcropping carbonate deposits at the northern rim of the Taoudeni Basin via the NE-trade winds leading to anomalously high percentages of calcite in the sand dunes (Fig. 9). Thus, the sand dunes may have also sourced the calcite present in the sample (Fig. 8b).

The winter sample of 2014-2015 was suggested to be sourced from sediments of the northern Senegal-Mauritania Basin (**PSA 2**) (Fig. 10a) and the eastern rim of the Taoudeni Basin (**PSA 3**) (Fig 10b). The palygorskite content of the sample (8 %) fits to the proposed bulk palygorskite content of **PSA 2** (Scheuvens et al., 2013). This points to several externally mixed sources during transport instead of single local source. The sample was further characterized by calcite and chlorite (Fig. 8b). The sediments in the northern Senegal-Mauritania Basin (Fig. 10a) comprise Quaternary chalky horizons (Wissmann, 1982) which may have sourced the calcite. More likely, calcite may have been derived from the Mesozoic carbonate sequences cropping out in the eastern rim of the Taoudeni Basin (Bertrand-Sarfati et al., 1991) (Fig. 10b). A source area lying at the Algerian/Mali border was also suggested for a chlorite and calcite bearing dust sample collected on the Canary Islands (Alastuey et al., 2005). The winter dust sample trapped at site Iwik was further characterized by the lowest feldspar percentage (~ 5 %), highest mica percentage (~ 40 %) (Fig. 8b) and lowest modal grain size (~ 38 µm) among all Iwik dust samples analysed for mineralogy. The Stokes terminal settling velocity is smaller for platy particles than for spherical particles of similar diameter (Santamarina and Cho, 2004). Therefore, a long-distance transport of dust from the eastern Taoudeni Basin to Iwik may have resulted in a depletion in spherical quartz particles (Fig. 5a,b,c) and an enrichment in platy mica particles (Fig. 5b).

The summer sample of 2013 was proposed to be sourced from the near-by northern Tidra Island (**PSA 2**) (Fig. 11a). Again, the absence of the mineral palygorskite is noteworthy which points to a single localized dust source. The sample was further characterized by the mineral gibbsite (Fig. 8c). The northern Tidra Island is famous for the local occurrence of west Africa's northernmost mangroves (Proske et al., 2008) which grow in humid and warm climates. Humid and warm conditions are also beneficial for the formation of gibbsite which forms through tropical weathering (Deer et al., 1992). Therefore, we argue that the soils of Tidra Island supplied the gibbsite found in the sample. A localized small gibbsite maximum was outlined for the surface sediments offshore Cape Blanc (Biscaye, 1964) which further supports the view that gibbsite is supplied from a local source. The sample was further characterized by anomalously large moderately spherical quartz grains (Fig. 5c) emphasizing a short travel distance of the dust.

The summer sample of 2014 was most likely sourced by sediments of the Western Sahara (**PSA 2**) (Fig. 12a,b). The palygorskite content of the sample (5 %) matches with the proposed bulk palygorskite content of **PSA 2** (Scheuvens et al., 2013). Hence, dust was supplied from several local dust sources of **PSA 2** which were mixed during transport. The sample was further characterized by calcite and dolomite (Fig. 8c). Sediments outcropping

in the Western Sahara are composed of Tertiary sediments (Wissmann, 1982) with limestone deposits (Bosse and Gwosdz, 1996) that may explain the calcite found in the sample (Fig., 12a). Upper cretaceous outcrops in the Aaiun-Tarfaya Basin near Laâyoune comprise dolomites (Bosse and Gwosdz, 1996) and could have sourced the dolomite found in the sample (Fig. 12b). A further evidence for dolomite-bearing dust transport from the Aaiun-Tarfaya Basin is a local dolomite maximum outlined for the surface sediments offshore the Western Sahara (Johnson, 1979). A Saharan dust sample trapped in NE Spain also contained dolomite and calcite and was related to a source area lying in the Western Sahara (Avila et al., 1997).

4.2.1 Dust collected at the marine sites

The seasonal contrast in the dust transport patterns (high-level Saharan Air Layer vs. low-level Trades) potentially leaded to strongly deviating dust sources for the material deposited in the marine trap samples. During winter, the back trajectories indicated that the potential dust source areas were located NE of the sampling site (Fig. 9b, Fig. 10c,d), while those during summer were located NE, E and SE of the sampling site (Fig. 11b, Fig.12a,c,d,e). This large variability in wind patterns can clearly be recognized in the clay-mineralogical compositions of the samples throughout the seasons.

Considering the much larger catchment area of the traps, several localized dust sources may have been sampled with the traps. As a result, the composition of the analyzed samples fit well to the bulk composition of the chosen **PSA**. The back trajectories indicate that the winter sample of 2014 originated from the shoreline of the Western Sahara (**PSA 2**) (Fig. 9b). The observed C/K ratio (C/K=1) and the palygorskite content (11 %) are in agreement with the bulk compositional C/K ratio (C/K=0-1) and palygorskite content of **PSA 2** (Scheuvens et al., 2013). The sample was further characterized by the presence of chlorite, kaolinite, smectite, garnet, anhydrite and fluellite (Fig. 8b). The characteristic occurrence of garnet together with the highest quartz content (33 %, Fig. 8b) among all CBi samples confirms a short transport distance of the trapped dust. Chlorite may be sourced from a small coastal area where chlorite-rich fluvisols are found (Journet et al., 2014) (Fig. 9b). The mineral fluellite which is a weathering product of phosphate may have been derived from outcropping phosphate deposits near the Bucraa phosphate mine (Moreno et al., 2006) (Fig. 9). The occurrence of kaolinite in the sample is remarkable as this mineral was not observed in high amounts in the soils underlying the back trajectories. However, the sample was further characterized by a lack of feldspar (Fig. 8b), which tends to be hydrothermally altered to kaolinite (Deer et al., 1992). The same process may explain the presence of anhydrite in this sample, although this mineral could also originate from evaporites along the coast. Another explanation for the presence of kaolinite and smectite may be the transport of these minerals from southern latitudes via the poleward-flowing undercurrent to the trap site CBi (Fig. 1). Kaolinite and smectite were found in the clay fraction of the surface sediments off Senegal (Nizou et al., 2011) and may have been brought into the ocean by the Senegal River, and redistributed by ocean currents (Biscaye, 1964). The season of high Senegal River sediment supply is between July to October/November (Gac and Kane, 1986). Assuming a mean speed of ~10 cm/s of the undercurrent (Mittelstaedt, 1991), it may take about two months for the particles to travel a distance of ~500 km to the trap site CBi. This time delay might explain the observed occurrence of these minerals in the trap samples during winter, but not during summer.

The back trajectories of the winter sample of 2014 to 2015 lead to the Reguibat Shield (**PSA 2) (**Fig. 10c) and coastal Western Sahara (**PSA 2)** (Fig. 10d). The observed C/K ratio (C/K=0) and palygorskite content (1 %) fall

790 within the ranges of these minerals in **PSA 2** (Scheuvens et al., 2013). The sample was further characterized by
791 the mineral zeolite (Fig. 8b). Zeolites are formed from volcanic glass and tuff and form well-developed crystals in
792 basalts (Deer et al., 1992). Therefore, the source area of the zeolites may have been outcropping volcanic rocks in
793 the northern Taoudeni Basin (Fig. 10c). These rocks belong to mafic dikes and sills which are commonly basalts
794 with dotted patches of glass (Verati et al., 2005). An additional indication for a distant dust source may be the
795 lowest quartz content (4 %) among all samples (Fig. 8b). The CBi trap sample was further characterized by the
796 minerals sepiolite and smectite (Fig. 8b). Sepiolite belongs to the pyrophyllites which is a mineral that also may
797 be considered indicative of tropical weathering (Moore and Reynolds, 1989). Similar to the winter dust sample
798 recovered during 2014, sepiolite and smectite may have been derived from humid weathering on the wet shoreline
799 of the Western Sahara (Fig. 10d) or from current transport of clay particles from the Senegal River mouth.
800 Palygorskite-sepiolite mafic clays were found in soil samples of the Western Sahara (Moreno et al., 2006) which
801 may supports a Western Saharan source.
802
803 Based on the back trajectories, the summer sample of 2013 was suggested to be sourced from the Mauritanides
804 (**PSA 2)** (Fig. 11c). This is confirmed by the palygorskite content of the sample (2 %) (Scheuvens et al., 2013).
805 Outstanding minerals in this sample are chlorite and rutile (Fig. 8c). Outcrops in the Mauritanides west of the
806 Taoudeni Basin feature strongly metamorphosed rocks (Villeneuve, 2005) and greenschist facies (Dallmeyer and
807 Lécorché, 2012) which may have been the source of the rutile and chlorite.
808
809 The reconstructed source area of the summer sample of 2014 was the Pharusian belt (**PSA 3)** (Fig. 12c) and the
810 extrusive volcanics of the northern Taoudeni Basin (**PSA 2)** (Fig. 12d). The lack of palygorskite in the sample
811 does corroborate with **PSA 4** ('not detected') (Scheuvens et al., 2013) suggesting that the provenance of the dust
812 sample may be mainly confined to **PSA 4**. The sample was further characterized by zeolite and ferryglaucophane
813 (Fig. 8c). The dike swarms and sills of the northern Taoudeni Basin (Verati et al., 2005) (Fig. 10c, Fig. 12c) and/or
814 the basalts of the Fezzan uplift (Fig. 12e) may have sourced the zeolite. Indeed, zeolite was described as one of
815 the main secondary minerals in the basaltic rocks of the central Al-Harui Al-Abyas basalt flows (Abdel-Karim et
816 al., 2013) and in vesicles of the east Al Haruj basalts (Cvetković et al., 2010) of the Fezzan uplift. Traces of zeolite
817 were also detected in the Iwik sample during this sampling interval. It may be that the zeolite dropped out of the
818 high-altitude dust cloud and was subsequently transported via the surface trade winds to the continental trap site.
819 The presence of ferryglaucophane and the absence of feldspar and chorite in the sample indicates highly
820 metamorphous outcrops constituting the dust source. Therefore, the sample may have been additionally sourced
821 by the Pharusian belt (Fig. 12c) because blueschists were observed in Timétrine (Caby, 2014) and glaucophane
822 bearing eclogites in the Gourma fold and thrust belt north of Gao (Caby et al., 2008). The sample was further
823 characterized by the highest mica content (44 %) among all samples (Fig. 8c) supporting a large dust transport
824 distance.
825
826
827
828

5. Summary and conclusions

The fluxes, grain-size distributions and the mineral assemblages of the continental trap samples and oceanic sediment trap samples were well comparable to the characteristics of Saharan dust reported for the region. The following main findings were made:

- dust deposited on the continent was predominantly transported with the trade winds from proximal sources, while dust deposited in the marine traps was transported with both the trade winds (winter, proximal) and in the Saharan Air Layer (summer, distal) from proximal and distal sources
- the percentage of mica relative to the quartz content increased in the deposited dust with increasing transport distance, most likely due to the platy shape of these minerals, which reduces settling

To conclude, the particle size and mineralogy of Saharan dust recorded in continental climate archives should be interpreted differently with respect to paleo-environmental conditions compared to marine climate archives; the on-land archive seems to reflect a much more local signal as compared to the regional signal that is recorded in the marine sediments. Given the relationship between particle size and wind strength, we suggest that the particle size in the continental archive in NW Africa may indicate the paleo-wind strength of the trade winds. This is an intuitively logical conclusion, but it has not been demonstrated before so clearly. Finally, we have shown how the mineralogical composition of the samples can be used for provenancing of dust particles found in both on-land and marine dust archives.

Atmos. Chem. Phys. Discuss., doi:10.5194/acp-2017-131, 2017
Manuscript under review for journal Atmos. Chem. Phys.
Discussion started: 16 February 2017

Atmospheric Chemistry and Physics Discussions

6. Appendices

A1 Satellite RGB images

In Fig. A1-4 satellite RGB true colour images are shown of the identified dust storms occurring during the sampling interval of the samples analysed for dust provenance. On 31 July 2014 only few dust can be observed which overlies the sampling location CBi (Fig. A2). This fits to the observed minor percentage of the mineral ferryglaucophane (7 %) in the sample which was suggested to be sourced on 31 July 2014 from PSA 3. Zeolite, which was more abundant (22 %) in the dust sample, was therefore most likely derived from PSA 4 due to the major dust storm event occurring on 7 August 2014 (Fig. A3).

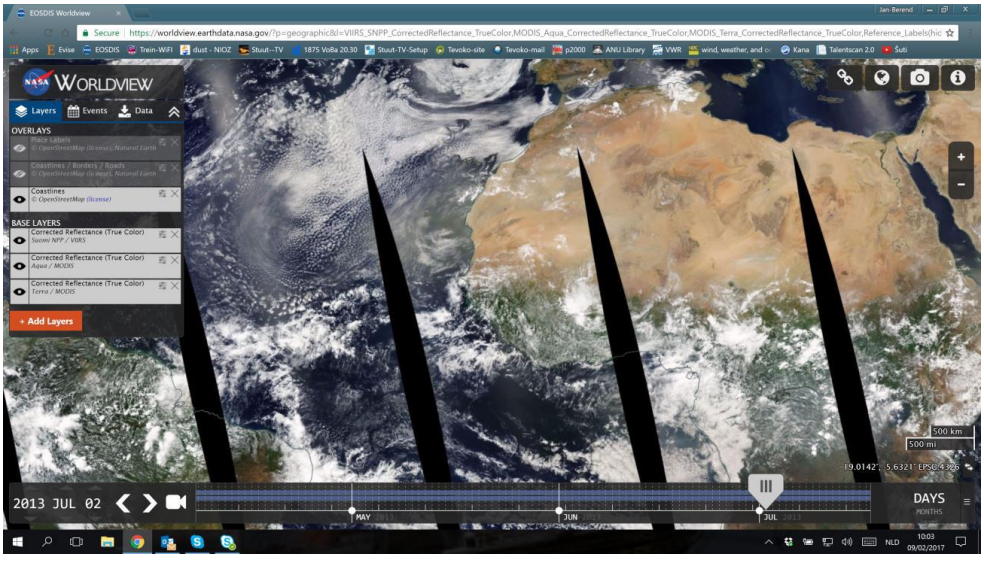

Figure A1: Dust storm on 02 July 2013.

Atmos. Chem. Phys. Discuss., doi:10.5194/acp-2017-131, 2017
Manuscript under review for journal Atmos. Chem. Phys.
Discussion started: 16 February 2017

Atmospheric Chemistry and Physics Discussions

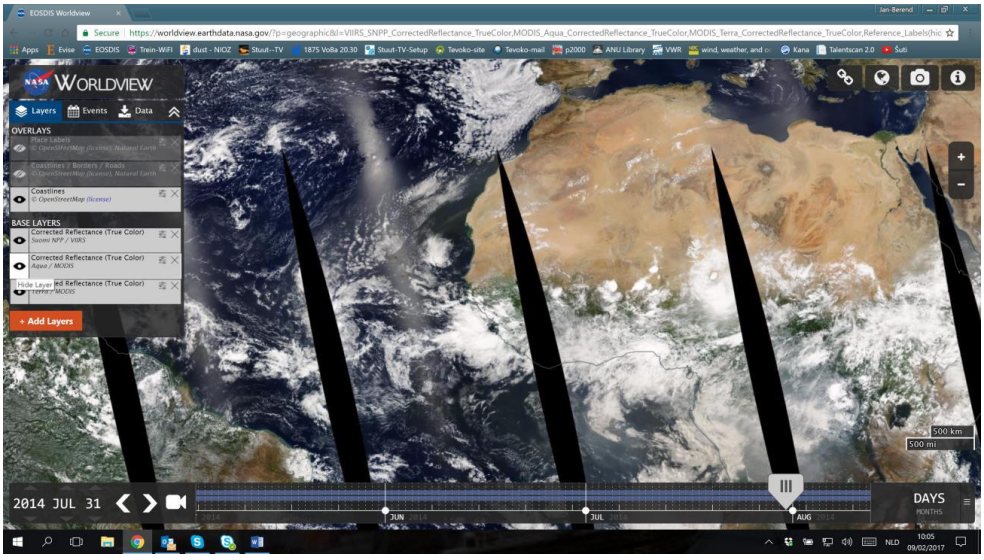

Figure A2: Dust storm on 31 July 2014.

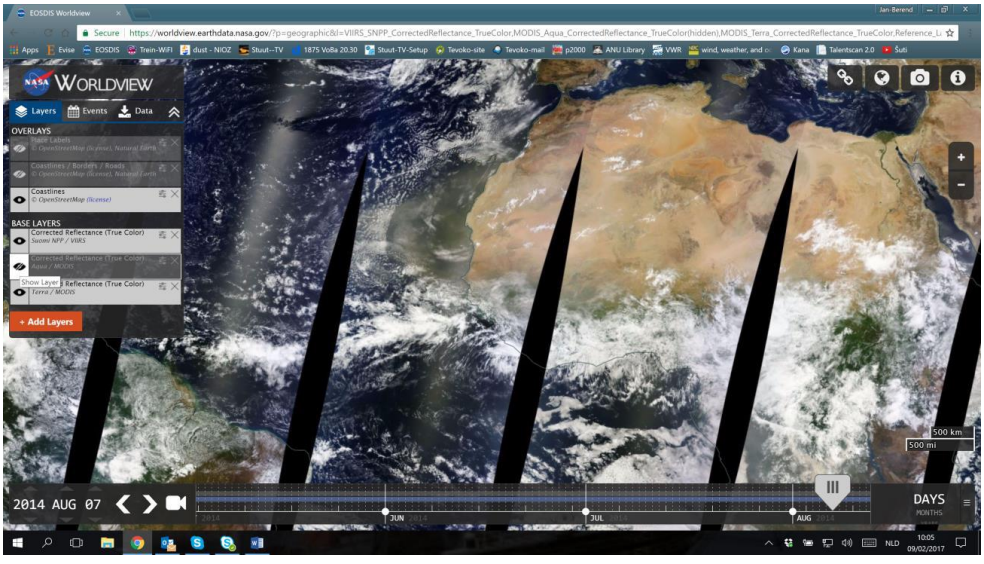

Figure A3: Dust storm on 07 August 2014.

Atmos. Chem. Phys. Discuss., doi:10.5194/acp-2017-131, 2017
Manuscript under review for journal Atmos. Chem. Phys.
Discussion started: 16 February 2017

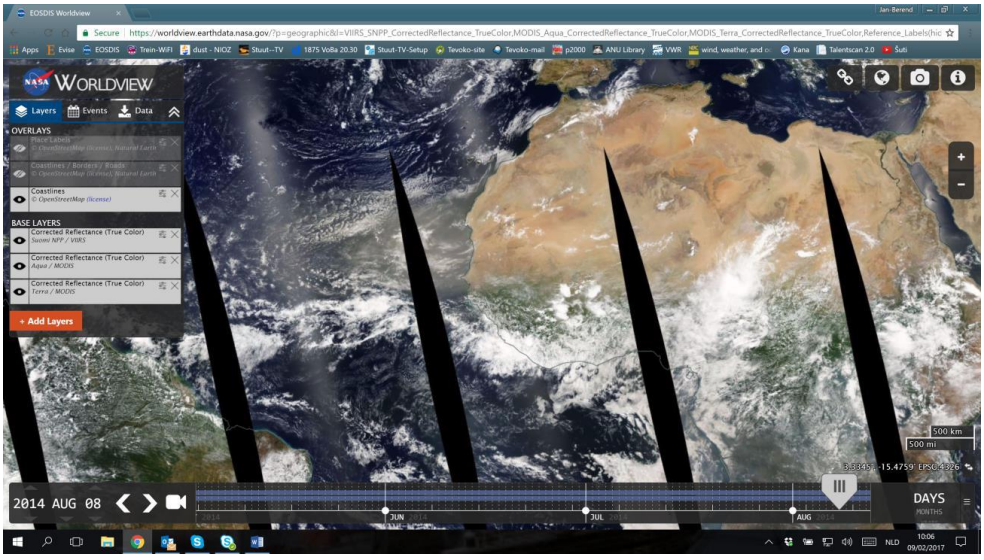

Figure A4: Dust storm on 08 August 2014.

A2 Four day back-trajectories

In Fig. A5-8 the four day back-trajectories are shown calculated at the heights 3000 m, 4500 m and 5500 m ending at site CBi. These high altitude back-trajectories were calculated for the identified summer days with dust storm events (shown in Fig A1-4). On the one hand, a height of 4500 m was chosen by Skonieczny et al. (2013) in a dust provenance study to represent the Saharan air layer (SAL). On the other hand, a height of 5500 m was chosen by Ratmeyer et al. (1999a) in a dust transport study to represent the SAL. Maximum wind velocities within the SAL are observed at a height of ~ 3 - 4 km in the area of the Cape Verde Islands during summer according to Carlson and Prospero (1972). Therefore, we also plotted the back-trajectories at a height of 3000 m. In order to investigate which air layer should be chosen for provenance studies, the back trajectories of the different heights were compared.

The back-trajectories deviated slightly from each other regarding their direction and length. The back-trajectories at 3000 m showed the most deviation. Further, the back-trajectories at 4500 m showed the best agreement with the source areas and the minerals in the samples. Therefore, we chose to use the trajectories at 4500 m for provenance studies according to Skonieczny et al. (2013).

Atmos. Chem. Phys. Discuss., doi:10.5194/acp-2017-131, 2017
Manuscript under review for journal Atmos. Chem. Phys.
Discussion started: 16 February 2017

Atmospheric Chemistry and Physics Discussions

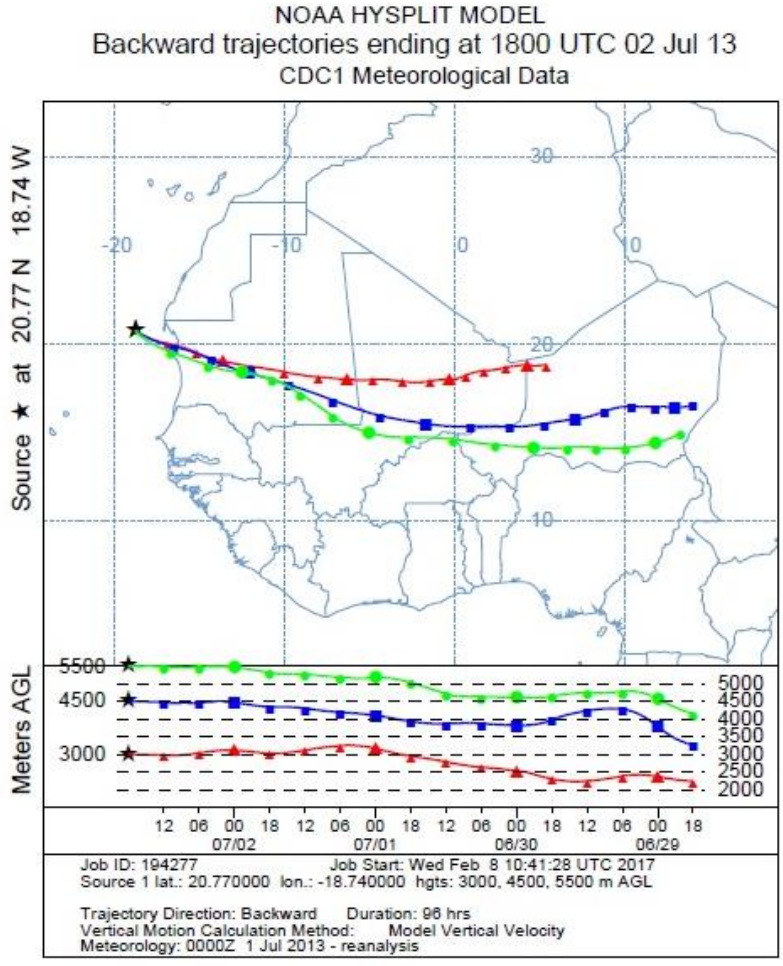

Figure A5: Four day back-trajectories at a height of 3000 m, 4500 m and 5500 m on 02 July 2013.

Atmos. Chem. Phys. Discuss., doi:10.5194/acp-2017-131, 2017
Manuscript under review for journal Atmos. Chem. Phys.
Discussion started: 16 February 2017

Atmospheric Chemistry and Physics Discussions

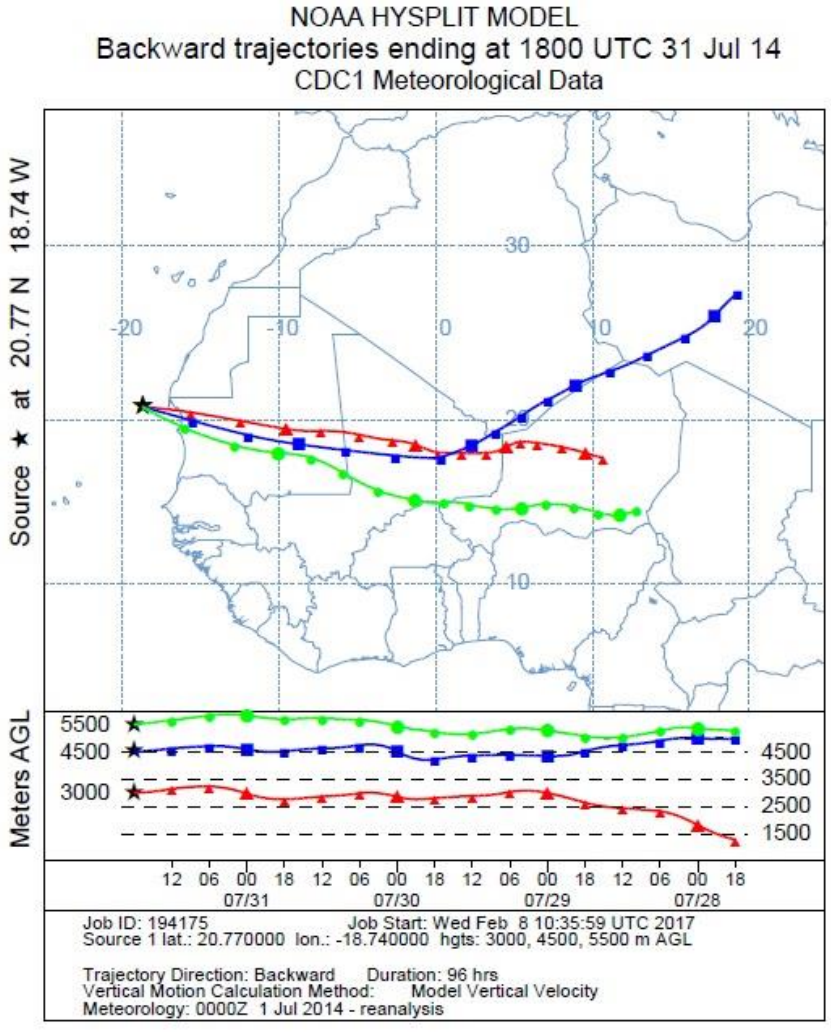

Figure A6: Four day back-trajectories at a height of 3000 m, 4500 m and 5500 m on 31 July 2014.

Atmos. Chem. Phys. Discuss., doi:10.5194/acp-2017-131, 2017
Manuscript under review for journal Atmos. Chem. Phys.
Discussion started: 16 February 2017

Atmospheric Chemistry and Physics Discussions

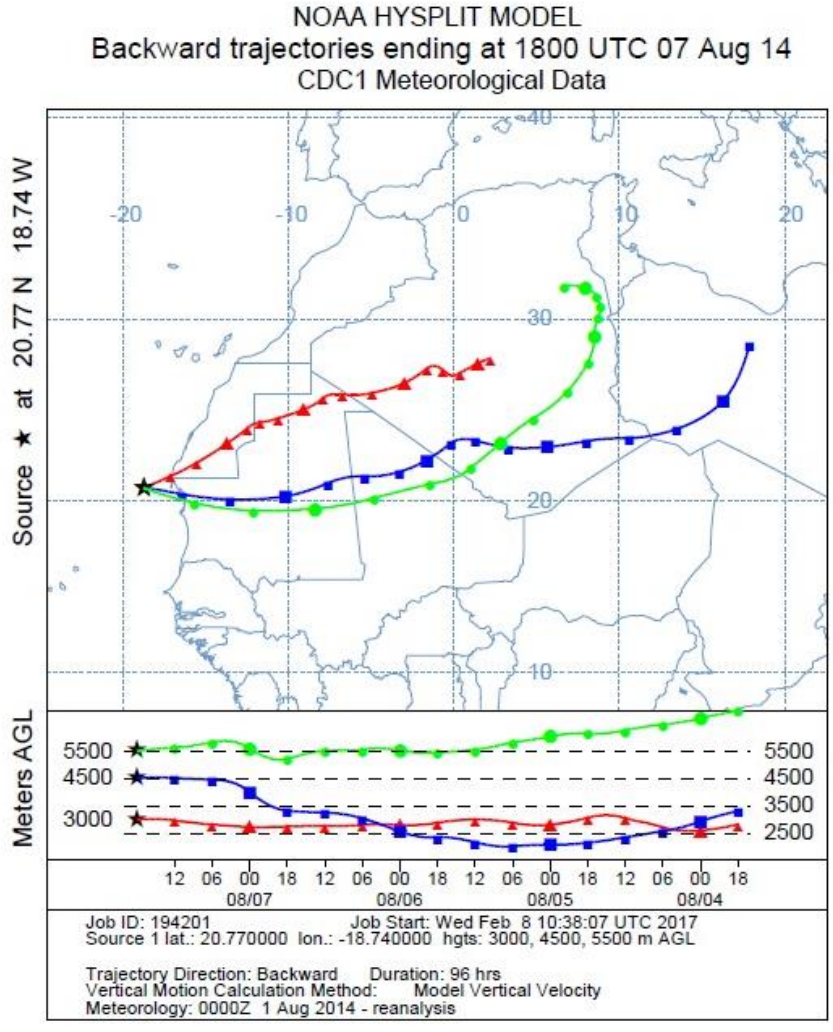

904

905 **Figure A7: Four day back-trajectories at a height of 3000 m, 4500 m and 5500 m on 07 August 2014.**

Atmos. Chem. Phys. Discuss., doi:10.5194/acp-2017-131, 2017
Manuscript under review for journal Atmos. Chem. Phys.
Discussion started: 16 February 2017

Atmospheric Chemistry and Physics Discussions

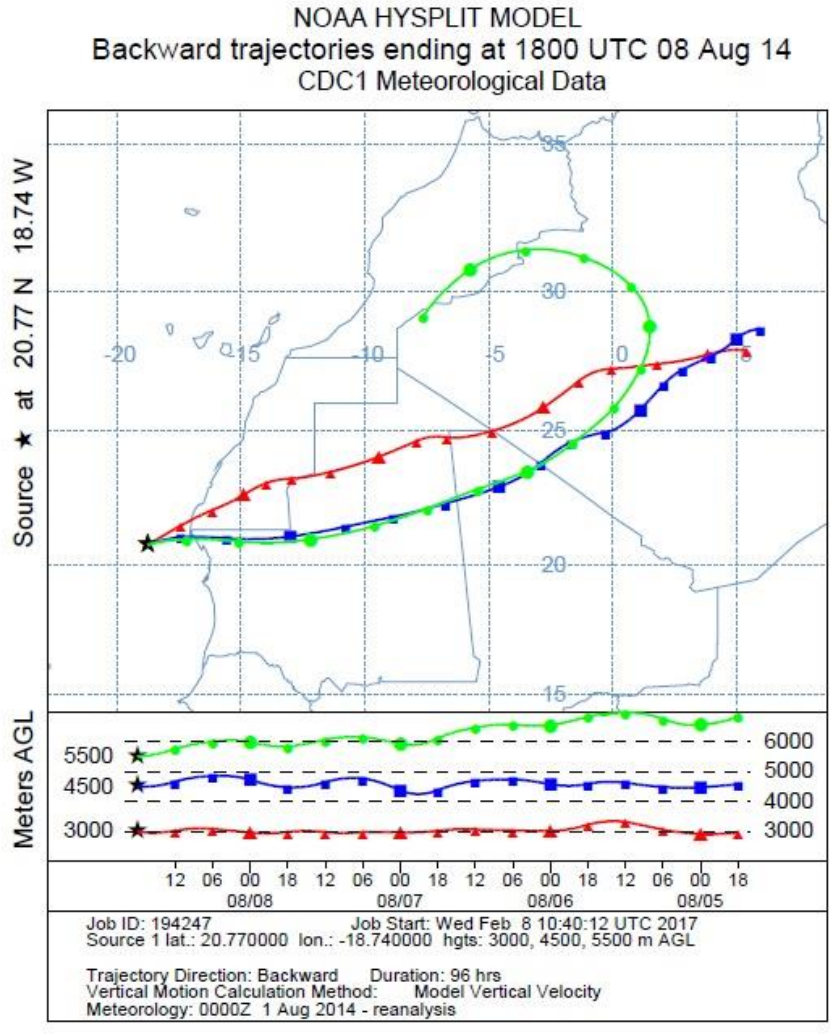

Figure A8: Four day back-trajectories at a height of 3000 m, 4500 m and 5500 m on 08 August 2014.

7. Supplement link

The data can be accessed on www.pangaea.de.

8. Author contribution

C. Friese carried out the particle size analysis of the sediment trap samples. H. van Hateren carried out the flux and particle size analysis of the Iwik dust samples. G. Fischer provided the sediment trap samples and supervised the flux analysis of the sediment trap samples. C. Friese prepared the samples for XRD analysis. C. Vogt carried out the XRD analysis and was involved in the discussion of the results. J.-B. Stuut managed the projects through

which dust-collecting buoy 'Carmen' was constructed and deployed, supervised the particle-size analysis and the writing of the manuscript. C. Friese prepared the manuscript with contributions from all co-authors.

9. Competing interests

The authors declare that they have no conflict of interest.

10. Acknowledgements

We thank the captains, crews and scientific teams of the research cruises with RV Poseidon in 2013 (POS445), RV Poseidon in 2014 (POS464) and RV Poseidon in 2015 (POS481), during which the sediment traps were deployed and received. Further, we thank Marco Klann for preparing and splitting the sediment trap samples. Jan-Berend Stuut acknowledges funding from ERC Grant 311152 DUSTTRAFFIC. Funding is acknowledged from the German Science Foundation (DFG) through the DFG-Research Center/Cluster of Excellence 'The Ocean in the Earth System'. We further thank Prof. Dr. Dierk Hebbeln and Dr. Ute Merkel for helpful and productive scientific discussions.

11. References

Abdel-Karim, A.-A. M., Ramadan, E.-N. M., and Embashi, M. R.: Multiphase Alkaline Basalts of Central Al-Haruj Al-Abyad of Libya: Petrological and Geochemical Aspects, Journal of Geological Research, 2013, 12, 10.1155/2013/805451, 2013.

Alastuey, A., Querol, X., Castillo, S., Escudero, M., Avila, A., Cuevas, E., Torres, C., Romero, P.-M., Exposito, F., and García, O.: Characterisation of TSP and PM2. 5 at Izana and Sta. Cruz de Tenerife (Canary Islands, Spain) during a Saharan Dust Episode (July 2002), Atmospheric Environment, 39, 4715-4728, 2005.

Aston, S. R., Chester, R., Johnson, L. R., and Padgham, R. C.: Eolian dust from the lower atmosphere of the eastern Atlantic and Indian oceans, China Sea and Sea of Japan, Marine Geology, 14, 15-28, 1973.

Avila, A., Queralt-Mitjans, I., and Alarcon, M.: Mineralogical composition of African dust delivered by red rains over northeastern Spain, Journal of Geophysical Research, 102, 21977-21996, 1997.

Bertrand-Sarfati, J., Moussine-Pouchkine, A., Affaton, P., Trompette, R., and Bellion, Y.: Cover sequences of the West African craton, in: The West African orogens and circum-Atlantic correlatives, Springer, 65-82, 1991.

Biscaye, P.: Mineralogy and sedimentation of recent Deep-sea clay in the Atlantic Ocean and adjacent seas and oceans., Geol Soc Am Bull, 76, 803-832, 1965.

Biscaye, P. E.: Mineralogy and sedimentation of the deep-sea sediment fine fraction in the Atlantic Ocean and adjacent seas and oceans, Ph.D., Geology, Yale University, Michigan, 86 pp., 1964.

Bloemsma, M. R., Zabel, M., Stuut, J. B. W., Tjallingii, R., Collins, J. A., and Weltje, G. J.: Modelling the joint variability of grain size and chemical composition in sediments, Sedimentary Geology, 280, 135-148, http://dx.doi.org/10.1016/j.sedgeo.2012.04.009, 2012.

Bory, A. J. M., and Newton, P. P.: Transport of airborne lithogenic material down through the water column in two contrasting regions of the eastern subtropical North Atlantic Ocean, Global Biogeochem. Cycles, 14, 297-315, 10.1029/1999gb900098, 2000.

Bosse, H.-R., and Gwosdz, W.: Limestone and dolomite resources of Africa, Geologisches Jahrbuch Reihe D, 500, 102, 1996.

Boullier, A.-M.: The pan-African trans-Saharan belt in the Hoggar shield (Algeria, Mali, Niger): A review, in: The west African orogens and circum-Atlantic correlatives, Springer, 85-105, 1991.

Caby, R., Buscail, F., Dembele, D., Diakite, S., Sacko, S., and Bal, M.: Neoproterozoic garnet-glaucophanites and eclogites: new insights for subduction metamorphism of the Gourma fold and thrust belt (eastern Mali), Geological Society, London, Special Publications, 297, 203-216, 2008.

961 Caby, R.: Nature and evolution of Neoproterozoic ocean-continent transition: Evidence from the
962 passive margin of the West African craton in NE Mali, Journal of African Earth Sciences, 91, 1-11,
963 http://dx.doi.org/10.1016/j.jafrearsci.2013.11.004, 2014.
964 Caquineau, S., Gaudichet, A., Gomes, L., and Legrand, M.: Mineralogy of Saharan dust transported
965 over northwestern tropical Atlantic Ocean in relation to source regions, Journal of Geophysical
966 Research, 107, 4251, 2002.
967 Carlson, T. N., and Prospero, J. M.: The Large-Scale Movement of Saharan Air Outbreaks over the
968 Northern Equatorial Atlantic, Journal of Applied Meteorology, 11, 283-297, 1972.
969 Chappell, A., Warren, A., O'Donoghue, A., Robinson, A., Thomas, A., and Bristow, C.: The
970 implications for dust emission modeling of spatial and vertical variations in horizontal dust flux and
971 particle size in the Bodélé Depression, Northern Chad, Journal of Geophysical Research:
972 Atmospheres, 113, n/a-n/a, 10.1029/2007JD009032, 2008.
973 Chester, R., Elderfield, H., and Griffin, J. J.: Dust transported in the North-east and South-east Trade
974 Winds in the Atlantic Ocean, Nature, 233, 474-476, 10.1038/233474a0, 1971.
975 Chester, R., and Johnson, L. R.: Atmospheric dusts collected off the West African Coast, Nature, 229,
976 105-107, 1971a.
977 Chester, R., and Johnson, L. R.: Atmospheric dusts collected off the Atlantic coasts of North Africa
978 and the Iberian Peninsula, Marine Geology, 11, 251-260, 1971b.
979 Chester, R., Elderfield, H., Griffin, J., Johnson, L., and Padgham, R.: Eolian dust along the eastern
980 margins of the Atlantic Ocean, Marine Geology, 13, 91-105, 1972.
981 Chung, F. H.: Quantitative interpretation of X-ray diffraction patterns of mixtures. I. Matrix-flushing
982 method for quantitative multicomponent analysis, Journal of Applied Crystallography, 7, 519-525,
983 1974.
984 Cropper, T. E., Hanna, E., and Bigg, G. R.: Spatial and temporal seasonal trends in coastal upwelling
985 off Northwest Africa, 1981–2012, Deep Sea Research Part I: Oceanographic Research Papers, 86, 94-
986 111, http://dx.doi.org/10.1016/j.dsr.2014.01.007, 2014.
987 Cvetković, V., Toljić, M., Ammar, N. A., Rundić, L., and Trish, K. B.: Petrogenesis of the eastern part
988 of the Al Haruj basalts (Libya), Journal of African Earth Sciences, 58, 37-50,
989 http://dx.doi.org/10.1016/j.jafrearsci.2010.01.006, 2010.
990 Dallmeyer, R. D., and Lécorché, J.-P.: The West African orogens and circum-Atlantic correlatives,
991 Springer Science & Business Media, 2012.
992 Deer, W. A., Howie, R. A., and Zussman, J.: An introduction to the rock-forming minerals, Longman
993 Scientific & Technical, 1992.
994 Delany, A. C., Claire Delany, A., Parkin, D. W., Griffin, J. J., Goldberg, E. D., and Reimann, B. E. F.:
995 Airborne dust collected at Barbados, Geochimica et Cosmochimica Acta, 31, 885-909, 1967.
996 Diaz, H. F., Carlson, T. N., Prospero, J. M., and Office, E. R. L. W. M. P.: A Study of the Structure
997 and Dynamics of the Saharan Air Layer Over the Northern Equatorial Atlantic During BOMEX, Nr.
998 32, Weather Modification Program Office, Environmental Research Laboratories, 1976.
999 Diester-Haass, L., and Chamley, H.: Neogene paleoenvironment off NW Africa based on sediments
1000 from DSDP Leg 14, Journal of Sedimentary Research, 48, 1978.
1001 Dobson, M.: An account of the Harmattan, a singular African wind, Philosophical transactions of the
1002 Royal Society of London, 71, 46-57, 1781.
1003 Einsele, G., Herm, D., and Schwarz, H. U.: Sea level fluctuation during the past 6000 yr at the coast of
1004 Mauritania, Quaternary Research, 4, 282-289, http://dx.doi.org/10.1016/0033-5894(74)90017-9, 1974.
1005 El Makkrouf, A. A.: Tectonic interpretation of Jabal Eghei area and its regional application to Tibesti
1006 orogenic belt, south central Libya (S.P.L.A.J.), Journal of African Earth Sciences (and the Middle
1007 East), 7, 945-967, http://dx.doi.org/10.1016/0899-5362(88)90009-7, 1988.
1008 Filipsson, H. L., Romero, O. E., Stuut, J.-B. W., and Donner, B.: Relationships between primary
1009 productivity and bottom-water oxygenation off northwest Africa during the last deglaciation, Journal
1010 of Quaternary Science, 26, 448-456, DOI:10.1002/jqs.1473, 2011.
1011 Fischer, G., and Wefer, G.: Sampling, Preparation and Analysis of Marine Particulate Matter, Geoph
1012 Monog Series, 63, 391-397, 1991.
1013 Fischer, G., and Karakas, G.: Sinking rates and ballast composition of particles in the Atlantic Ocean:
1014 implications for the organic carbon fluxes to the deep ocean, Biogeosciences, 6, 85-102, 2009.

1015 Fischer, G., Ba, M., Dehning, K., Hefter, J., Iversen, M., Klann, M., Nowald, N., Ploug, H., Ruhland,
1016 G., and Witte, Y.: Report and preliminary results of R/V POSEIDON cruise POS445. Las Palmas–Las
1017 Palmas, 19.01. 2013–01.02. 2013, 2013.
1018 Fischer, G., Dehning, K., Dia, A., Füssel, J., Hefter, J., Iversen, M., Klann, M., Nowald, N., Olbrich,
1019 M., and Ruhland, G.: Report and preliminary results of RV POSEIDON cruise POS464, Las Palmas
1020 (Canary Islands)-Las Palmas (Canary Islands), 03.02. 2014-18.02. 2014, 2014.
1021 Fischer, G., Dia, A., Iversen, M., Klann, M., Nowald, N., Markussen, T., Meckel, S., Ruhland, G., Van
1022 der Jagt, H., and Waldmann, C.: Report and preliminary results of R/V POSEIDON cruise POS481,
1023 Las Palmas (Canary Islands)-Las Palmas (Canary Islands), 15.03. 2015-03.03. 2015, 2015a.
1024 Fischer, G., Romero, O., Merkel, U., Donner, B., Iversen, M., Nowald, N., Ratmeyer, V., Ruhland, G.,
1025 Klann, M., and Wefer, G.: Deep ocean mass fluxes in the coastal upwelling off Mauritania from 1988
1026 to 2012: variability on seasonal to decadal timescales, Biogeosciences Discussions, 12, 2015b.
1027 Formenti, P., Rajot, J. L., Desboeufs, K., Caquineau, S., Chevaillier, S., Nava, S., Gaudichet, A.,
1028 Journet, E., Triquet, S., Alfaro, S., Chiari, M., Haywood, J., Coe, H., and Highwood, E.: Regional
1029 variability of the composition of mineral dust from western Africa: Results from the AMMA
1030 SOP0/DABEX and DODO field campaigns, Journal of Geophysical Research: Atmospheres, 113, n/a-
1031 n/a, 10.1029/2008JD009903, 2008.
1032 Friese, C. A., van der Does, M., Merkel, U., Iversen, M. H., Fischer, G., and Stuut, J.-B. W.:
1033 Environmental factors controlling the seasonal variability in particle size distribution of modern
1034 Saharan dust deposited off Cape Blanc, Aeolian Research, 22, 165-179,
1035 http://dx.doi.org/10.1016/j.aeolia.2016.04.005, 2016.
1036 Fütterer, D.: Sedimentation am NW-afrikanischen Kontinentalrand: Quantitative Zusammensetzung
1037 und Verteilung der Siltfraktion in den Oberflächensedimenten, Meteor-Forschungsergebnisse, C, 15-
1038 60, 1980.
1039 Gac, J. Y., and Kane, A.: Le Fleuve Sénégal: I. Bilan hydrologique et flux continentaux de matières
1040 particulaires a l'embouchure, Sci. Géol. Bull., 39, 99-130, 1986.
1041 Gillies, J. A., Nickling, W. G., and McTainsh, G. H.: Dust concentrations and particle-size
1042 characteristics of an intense dust haze event: inland delta region, Mali, West Africa, Atmospheric
1043 Environment, 30, 1081-1090, 1996.
1044 Glaccum, R. A., and Prospero, J. M.: Saharan aerosols over the tropical North Atlantic - mineralogy,
1045 Marine Geology, 37, 295-321, 1980.
1046 Goossens, D., and Offer, Z. Y.: Wind tunnel and field calibration of six aeolian dust samplers,
1047 Atmospheric Environment, 34, 1043-1057, 10.1016/s1352-2310(99)00376-3, 2000.
1048 Goossens, D.: Relationships between horizontal transport flux and vertical deposition flux during dry
1049 deposition of atmospheric dust particles, Journal of Geophysical Research: Earth Surface, 113, n/a-n/a,
1050 10.1029/2007JF000775, 2008.
1051 Griffin, J. J., Windom, H., and Goldberg, E. D.: The distribution of clay minerals in the World Ocean,
1052 Deep Sea Research and Oceanographic Abstracts, 15, 433-459, http://dx.doi.org/10.1016/0011-
1053 7471(68)90051-X, 1968.
1054 Haywood, J., and Boucher, O.: Estimates of the direct and indirect radiative forcing due to
1055 tropospheric aerosols: A review, Rev Geophys, 38, 513-543, Doi 10.1029/1999rg000078, 2000.
1056 Holz, C., Stuut, J.-B. W., and Henrich, R.: Terrigenous sedimentation processes along the continental
1057 margin off NW-Africa: implications from grain-size analyses of surface sediments, Sedimentology,
1058 51, 1145-1154, .1111/j.1365-3091.2004.00665.x, 2004.
1059 Holz, C., Stuut, J.-B. W., Henrich, R., and Meggers, H.: Variability in terrigenous sedimentation
1060 processes off northwest Africa and its relation to climate changes: Inferences from grain-size
1061 distributions of a Holocene marine sediment record, Sedimentary Geology, 202, 499-508,
1062 10.1016/j.sedgeo.2007.03.015, 2007.
1063 Iversen, M. H., Nowald, N., Ploug, H., Jackson, G. A., and Fischer, G.: High resolution profiles of
1064 vertical particulate organic matter export off Cape Blanc, Mauritania: Degradation processes and
1065 ballasting effects, Deep Sea Research Part I: Oceanographic Research Papers, 57, 771-784, DOI:
1066 10.1016/j.dsr.2010.03.007, 2010.
1067 Iversen, M. H., and Ploug, H.: Ballast minerals and the sinking carbon flux in the ocean: carbon-
1068 specific respiration rates and sinking velocities of macroscopic organic aggregates (marine snow),
1069 Biogeosciences Discuss., 7, 3335-3364, 10.5194/bgd-7-3335-2010, 2010.

1070 Iversen, M. H., and Robert, M. L.: Ballasting effects of smectite on aggregate formation and export
1071 from a natural plankton community, Marine Chemistry, 175, 18-27,
1072 http://dx.doi.org/10.1016/j.marchem.2015.04.009, 2015.
1073 Jickells, T. D., An, Z. S., Andersen, K. K., Baker, A. R., Bergametti, G., Brooks, N., Cao, J. J., Boyd,
1074 P. W., Duce, R. A., Hunter, K. A., Kawahata, H., Kubilay, N., laRoche, J., Liss, P. S., Mahowald, N.,
1075 Prospero, J. M., Ridgwell, A. J., Tegen, I., and Torres, R.: Global Iron Connections Between Desert
1076 Dust, Ocean Biogeochemistry, and Climate, Science, 308, 67-71, 2005.
1077 Johnson, L. R.: Mineralogical dispersal patterns of North Atlantic deep-sea sediments with particular
1078 reference to eolian dusts, Marine Geology, 29, 335-345, http://dx.doi.org/10.1016/0025-
1079 3227(79)90115-4, 1979.
1080 Journet, E., Balkanski, Y., and Harrison, S. P.: A new data set of soil mineralogy for dust-cycle
1081 modeling, Atmos. Chem. Phys., 14, 3801-3816, 10.5194/acp-14-3801-2014, 2014.
1082 Kandler, K., Schütz, L., Deutscher, C., Ebert, M., Hofmann, H., Jäckel, S., Jaenicke, R., Knippertz, P.,
1083 Lieke, K., Massling, A., Petzold, A., Schladitz, A., Weinzierl, B., Wiedensohler, A., Zorn, S., and
1084 Weinbruch, S.: Size distribution, mass concentration, chemical and mineralogical composition and
1085 derived optical parameters of the boundary layer aerosol at Tinfou, Morocco, during SAMUM 2006,
1086 Tellus B, 61, 32-50, 10.1111/j.1600-0889.2008.00385.x, 2009.
1087 Khiri, F., Ezaidi, A., and Kabbachi, K.: Dust deposits in Souss-Massa basin, South-West of Morocco:
1088 granulometrical, mineralogical and geochemical characterisation, Journal of African Earth Sciences,
1089 39, 459-464, 2004.
1090 Knippertz, P., and Todd, M. C.: Mineral dust aerosols over the Sahara: Meteorological controls on
1091 emission and transport and implications for modeling, Rev Geophys, 50, n/a-n/a,
1092 10.1029/2011RG000362, 2012.
1093 Knippertz, P., and Stuut, J.-B. W.: Mineral dust a key player in the Earth system, Springer, Dordrecht,
1094 2014.
1095 Koch, J., and Renno, N. O.: The role of convective plumes and vortices on the global aerosol budget,
1096 Geophysical Research Letters, 32, n/a-n/a, 10.1029/2005GL023420, 2005.
1097 Kogbe, C. A.: Geology of the upper cretaceous and tertiary sediments of the Nigerian sector of the
1098 Iullemeden Basin (West-Africa), Geol Rundsch, 62, 197-211, 10.1007/bf01826827, 1973.
1099 Koopmann, B.: Sedimentation von Saharastaub im subtropischen Nordatlantik während der letzten
1100 25.000 Jahre, Meteor Forschungsergebnisse C, 35, 23-59, 1981.
1101 Korte, L. F., Brummer, G. J., van der Does, M., Guerreiro, C. V., Hennekam, R., van Hateren, J. A.,
1102 Jong, D., Munday, C. I., Schouten, S., and Stuut, J. B. W.: Compositional changes of present-day
1103 transatlantic Saharan dust deposition, Atmos. Chem. Phys. Discuss., 2016, 1-24, 10.5194/acp-2016-
1104 1068, 2016.
1105 Lancaster, N.: 11.12 Sand Seas and Dune Fields A2 - Shroder, John F, in: Treatise on
1106 Geomorphology, Academic Press, San Diego, 219-245, 2013.
1107 Lange, H.: Herkunft und Vertei-lung von Oberflachensedimenten des westafrikanischen Schelfs und
1108 Kontinentalhanges.', "Meteor" Forschungsergeb, 22, 61-84, 1975.
1109 Lange, H.: Distribution of Chlorite and Kaolinite in Eastern Atlantic Sediments Off North-Africa,
1110 Sedimentology, 29, 427-431, DOI 10.1111/j.1365-3091.1982.tb01805.x, 1982.
1111 Lau, K. M., and Kim, K. M.: Cooling of the Atlantic by Saharan dust, Geophys. Res. Lett., 34,
1112 10.1029/2007GL031538, 2007.
1113 Martin, J. H.: Glacial-interglacial CO_2 change: the iron hypothesis, Paleoceanography, 5, 1-13, 1990.
1114 Martin, J. H., Gordon, R. M., and Fitzwater, S. E.: The case for iron, Limnology & Oceanography, 36,
1115 1793-1802, 1991.
1116 McTainsh, G. H., Nickling, W. G., and Lynch, A. W.: Dust deposition and particle size in Mali, West
1117 Africa, Catena, 29, 307-322, 1997.
1118 Mendez, M. J., Funk, R., and Buschiazzo, D. E.: Field wind erosion measurements with Big Spring
1119 Number Eight (BSNE) and Modified Wilson and Cook (MWAC) samplers, Geomorphology, 129, 43-
1120 48, 10.1016/j.geomorph.2011.01.011, 2011.
1121 Meunier, T., Barton, E. D., Barreiro, B., and Torres, R.: Upwelling filaments off Cap Blanc:
1122 Interaction of the NW African upwelling current and the Cape Verde frontal zone eddy field?, Journal
1123 of Geophysical Research: Oceans, 117, n/a-n/a, 10.1029/2012JC007905, 2012.

Meyer, I., Davies, G. R., Vogt, C., Kuhlmann, H., and Stuut, J.-B. W.: Changing rainfall patterns in NW Africa since the Younger Dryas, Aeolian Research, 10, 111-123, http://dx.doi.org/10.1016/j.aeolia.2013.03.003, 2013.

Mittelstaedt, E.: The ocean boundary along the northwest African coast: Circulation and oceanographic properties at the sea surface, Progress In Oceanography, 26, 307-355, 10.1016/0079-6611(91)90011-A, 1991.

Moore, D. M., and Reynolds, R. C.: X-ray Diffraction and the Identification and Analysis of Clay Minerals, Oxford university press Oxford, 1989.

Moreno, T., Querol, X., Castillo, S., Alastuey, A., Cuevas, E., Herrmann, L., Mounkaila, M., Elvira, J., and Gibbons, W.: Geochemical variations in aeolian mineral particles from the Sahara-Sahel Dust Corridor, Chemosphere, 65, 261-270, 2006.

Mulitza, S., Heslop, D., Pittauerova, D., Fischer, H. W., Meyer, I., Stuut, J.-B., Zabel, M., Mollenhauer, G., Collins, J. A., Kuhnert, H., and Schulz, M.: Increase in African dust flux at the onset of commercial agriculture in the Sahel region, Nature, 466, 226-228, 10.1038/nature09213, 2010.

National Geospatial-Intelligence Agency: North Atlantic, Baltic Sea, North Sea and Mediterranean Sea, 4 ed., Sailing directions (planning guide), ProStar Publications, 2006.

Nicholson, S. E.: A revised picture of the structure of the "monsoon" and land ITCZ over West Africa, Climate Dynamics, 32, 1155-1171, DOI 10.1007/s00382-008-0514-3, 2009.

Nizou, J., Hanebuth, T. J. J., and Vogt, C.: Deciphering signals of late Holocene fluvial and aeolian supply from a shelf sediment depocentre off Senegal (north-west Africa), Journal of Quaternary Science, n/a-n/a, 10.1002/jqs.1467, 2011.

Piqué, A.: Geology of northwest Africa, Gebrüder Borntraeger, 2001.

Ploug, H., Iversen, M. H., and Fischer, G.: Ballast, sinking velocity, and apparent diffusivity within marine snow and zooplankton fecal pellets: Implications for substrate turnover by attached bacteria, Limnology and Oceanography, 53, 1878-1886, 2008a.

Ploug, H., Iversen, M. H., Koski, M., and Buitenhuis, E. T.: Production, oxygen respiration rates, and sinking velocity of copepod fecal pellets: Direct measurements of ballasting by opal and calcite, Limnology and Oceanography, 53, 469-476, DOI 10.4319/lo.2008.53.2.0469, 2008b.

Proske, U., Hanebuth, T. J. J., Meggers, H., and Leroy, S. A. G.: Tidal flat sedimentation during the last millennium in the northern area of Tidra Island, Banc d'Arguin, Mauritania, Journal of African Earth Sciences, 50, 37-48, http://dx.doi.org/10.1016/j.jafrearsci.2007.09.002, 2008.

Prospero, J. M., and Carlson, T. N.: Radon-222 in North Atlantic Trade Winds . Its Relationship to Dust Transport from Africa, Science, 167, 974-&, Doi 10.1126/Science.167.3920.974, 1970.

Prospero, J. M., and Carlson, T. N.: Vertical and areal distribution of Saharan dust over the western equatorial north Atlantic Ocean, Journal of Geophysical Research, 77, 5255-5265, 10.1029/JC077i027p05255, 1972.

Prospero, J. M., Ginoux, P., Torres, O., Nicholson, S. E., and Gill, T. E.: Environmental characterization of global sources of atmospheric soil dust identified with the Nimbus 7 total ozone mapping spectrometer (TOMS) absorbing aerosol product, Rev Geophys, 40, 1-31, 2002.

Pye, K.: The nature, origin and accumulation of loess, Quaternary Science Reviews, 14, 653-667, 1995.

Radczewski, O. E.: Eolian deposits in marine sediments, 1939.

Rateev, M. A., Gorbunova, Z. N., Lisitzyn, A. P., and Nosov, G. L.: THE DISTRIBUTION OF CLAY MINERALS IN THE OCEANS, Sedimentology, 13, 21-43, 10.1111/j.1365-3091.1969.tb01119.x, 1969.

Ratmeyer, V., Balzer, W., Bergametti, G., Chiapello, I., Fischer, G., and Wyputta, U.: Seasonal impact of mineral dust on deep-ocean particle flux in the eastern subtropical Atlantic Ocean, Marine Geology, 159, 241-252, 1999a.

Ratmeyer, V., Fischer, G., and Wefer, G.: Lithogenic particle fluxes and grain size distributions in the deep ocean off northwest Africa: Implications for seasonal changes of aeolian dust input and downward transport, Deep Sea Research Part I: Oceanographic Research Papers, 46, 1289-1337, 1999b.

Rea, D. K.: The paleoclimatic record provided by eolian deposition in the deep sea: the geologic history of wind, Rev Geophys, 32, 159-195, 1994.

Santamarina, J., and Cho, G.: Soil behaviour: The role of particle shape, Advances in geotechnical engineering: The skempton conference, 2004, 604-617,

Scheuvens, D., Schütz, L., Kandler, K., Ebert, M., and Weinbruch, S.: Bulk composition of northern African dust and its source sediments — A compilation, Earth-Science Reviews, 116, 170-194, http://dx.doi.org/10.1016/j.earscirev.2012.08.005, 2013.

Schlüter, T.: Geological atlas of Africa, Springer, 2008.

Schofield, D., Horstwood, M., Pitfield, P., Crowley, Q., Wilkinson, A., and Sidaty, H. C. O.: Timing and kinematics of Eburnean tectonics in the central Reguibat Shield, Mauritania, Journal of the Geological Society, 163, 549-560, 2006.

Schuster, M., Duringer, P., Ghienne, J.-F., Roquin, C., Sepulchre, P., Moussa, A., Lebatard, A.-E., Mackaye, H. T., Likius, A., Vignaud, P., and Brunet, M.: Chad Basin: Paleoenvironments of the Sahara since the Late Miocene, Comptes Rendus Geoscience, 341, 603-611, http://dx.doi.org/10.1016/j.crte.2009.04.001, 2009.

Schütz, L., and Sebert, M.: Mineral aerosols and source identification, Journal of Aerosol Science, 18, 1-10, http://dx.doi.org/10.1016/0021-8502(87)90002-4, 1987.

Selley, R. C.: Chapter 1 The sedimentary basins of northwest africa: stratigraphy and sedimentation, in: Sedimentary Basins of the World, edited by: Selley, R. C., Elsevier, 3-16, 1997a.

Selley, R. C.: Chapter 2 The basins of northwest africa: Structural evolution, in: Sedimentary Basins of the World, edited by: Selley, R. C., Elsevier, 17-26, 1997b.

Selley, R. C.: Chapter 3 The sirte basin of libya, in: Sedimentary Basins of the World, edited by: Selley, R. C., Elsevier, 27-37, 1997c.

Skonieczny, C., Bory, A., Bout-Roumazeilles, V., Abouchami, W., Galer, S. J. G., Crosta, X., Stuut, J. B., Meyer, I., Chiapello, I., Podvin, T., Chatenet, B., Diallo, A., and Ndiaye, T.: The 7-13 March 2006 major Saharan outbreak: Multiproxy characterization of mineral dust deposited on the West African margin, J. Geophys. Res., 116, D18210, 10.1029/2011jd016173, 2011.

Skonieczny, C., Bory, A., Bout-Roumazeilles, V., Abouchami, W., Galer, S. J. G., Crosta, X., Diallo, A., and Ndiaye, T.: A three-year time series of mineral dust deposits on the West African margin: Sedimentological and geochemical signatures and implications for interpretation of marine paleo-dust records, Earth and Planetary Science Letters, 364, 145-156, http://dx.doi.org/10.1016/j.epsl.2012.12.039, 2013.

Stein, A. F., Draxler, R. R., Rolph, G. D., Stunder, B. J. B., Cohen, M. D., and Ngan, F.: NOAA's HYSPLIT Atmospheric Transport and Dispersion Modeling System, Bulletin of the American Meteorological Society, 96, 2059-2077, 10.1175/bams-d-14-00110.1, 2015.

Stein, R.: Late neogene changes of paleoclimate and paleoproductivity off northwest africa (D.S.D.P. Site 397), Palaeogeography, Palaeoclimatology, Palaeoecology, 49, 47-59, http://dx.doi.org/10.1016/0031-0182(85)90004-5, 1985.

Stuut, J.-B. W.: Late Quaternary Southwestern African terrestrial-climate signals in the marine record of Walvis Ridge, SE Atlantic Ocean, Faculty of Earth Sciences, Utrecht University, Utrecht, 128 pp., 2001.

Stuut, J.-B. W., Zabel, M., Ratmeyer, V., Helmke, P., Schefuß, E., Lavik, G., and Schneider, R. R.: Provenance of present-day eolian dust collected off NW Africa, Journal of Geophysical Research, 110, 10.1029/2004JD005161, 2005.

Stuut, J.-B. W., Bakker, M., Friese, C., Koster, B., Visser, J.-D. d., and Witte, Y.: Cruise Report and preliminary results - DUSTTRAFFIC: Transatlantic fluxes of Saharan dust - Cruise No. 64PE392 - 19 – 27 August 2014 Las Palmas de Gran Canaria (Spain) – Mindelo, Sao Vicente (Cape Verdian Islands), 2015.

Ternon, E., Guieu, C., Loÿe-Pilot, M. D., Leblond, N., Bosc, E., Gasser, B., Miquel, J. C., and Martín, J.: The impact of Saharan dust on the particulate export in the water column of the North Western Mediterranean Sea, Biogeosciences, 7, 809-826, 10.5194/bg-7-809-2010, 2010.

Tjallingii, R., Claussen, M., Stuut, J.-B. W., Fohlmeister, J., Jahn, A., Bickert, T., Lamy, F., and Rohl, U.: Coherent high- and low-latitude control of the northwest African hydrological balance, Nature Geoscience, 1, 670-675, 10.1038/ngeo289, 2008.

Tsoar, H., and Pye, K.: Dust transport and the question of desert loess formation, Sedimentology, 34, 139-153, 1987.

Tucker, M. E., and Tucker, M.: Techniques in sedimentology, 552.5. 08 TEC, 1988.

Van Camp, L., Nykjaer, L., Mittelstaedt, E., and Schlittenhardt, P.: Upwelling and boundary circulation off Northwest Africa as depicted by infrared and visible satellite observations, Progress in Oceanography, 26, 357-402, http://dx.doi.org/10.1016/0079-6611(91)90012-B, 1991.

1236 Van der Does, M., Korte, L. F., Munday, C. I., Brummer, G. J. A., and Stuut, J. B. W.: Particle size
1237 traces modern Saharan dust transport and deposition across the equatorial North Atlantic, Atmos.
1238 Chem. Phys. Discuss., 2016, 1-27, 10.5194/acp-2016-344, 2016a.
1239 Van der Does, M., Korte, L. F., Munday, C. I., Brummer, G. J. A., and Stuut, J. B. W.: Particle size
1240 traces modern Saharan dust transport and deposition across the equatorial North Atlantic, Atmos.
1241 Chem. Phys., 16, 13697-13710, 10.5194/acp-16-13697-2016, 2016b.
1242 Verati, C., Bertrand, H., and Féraud, G.: The farthest record of the Central Atlantic Magmatic
1243 Province into West Africa craton: Precise 40Ar/39Ar dating and geochemistry of Taoudenni basin
1244 intrusives (northern Mali), Earth and Planetary Science Letters, 235, 391-407,
1245 http://dx.doi.org/10.1016/j.epsl.2005.04.012, 2005.
1246 Villeneuve, M.: Paleozoic basins in West Africa and the Mauritanide thrust belt, Journal of African
1247 Earth Sciences, 43, 166-195, http://dx.doi.org/10.1016/j.jafrearsci.2005.07.012, 2005.
1248 Vogt, C., Lauterjung, J., and Fischer, R. X.: Investigation of the Clay Fraction (< 2 µm) of the Clay
1249 Minerals Society Reference Clays, Clays and Clay Minerals, 50, 388-400, 2002.
1250 Wilson, S., and Cooke, R.: Wind erosion, Soil erosion, 217251, 1980.
1251 Wissmann, G.: Stratigraphy and structural features of the continental margin basin of Senegal and
1252 Mauritania, in: Geology of the Northwest African continental margin, Springer, 160-181, 1982.
1253 Yoshioka, M., Mahowald, N. M., Conley, A. J., Collins, W. D., Fillmore, D. W., Zender, C. S., and
1254 Coleman, D. B.: Impact of Desert Dust Radiative Forcing on Sahel Precipitation: Relative Importance
1255 of Dust Compared to Sea Surface Temperature Variations, Vegetation Changes, and Greenhouse Gas
1256 Warming, Journal of Climate, 20, 1445-1467, doi:10.1175/JCLI4056.1, 2007.
1257 Yu, H. B., Chin, M., Bian, H. S., Yuan, T. L., Prospero, J. M., Omar, A. H., Remer, L. A., Winker, D.
1258 M., Yang, Y. K., Zhang, Y., and Zhang, Z. B.: Quantification of trans-Atlantic dust transport from
1259 seven-year (2007-2013) record of CALIPSO lidar measurements, Remote Sens Environ, 159, 232-
1260 249, 10.1016/j.rse.2014.12.010, 2015.
1261 Zobeck, T. M., Sterk, G., Funk, R., Rajot, J. L., Stout, J. E., and Van Pelt, R. S.: Measurement and
1262 data analysis methods for field-scale wind erosion studies and model validation, Earth Surface
1263 Processes and Landforms, 28, 1163-1188, 10.1002/esp.1033, 2003.

1264

1265